



The sources of volatile and fluid-mobile elements in the Sunda arc: A melt inclusion study from Kawah Ijen and Tambora volcanoes, Indonesia

Nathalie Vigouroux

Department of Earth Sciences, Simon Fraser University, Burnaby, British Columbia V5A 1S6, Canada

Alterra Power Corp., Vancouver, British Columbia V6C 3K4, Canada (nvigouroux@alterrapower.ca)

Paul J. Wallace

Department of Geological Sciences, University of Oregon, Eugene, Oregon 97403, USA

Glyn Williams-Jones

Department of Earth Sciences, Simon Fraser University, Burnaby, British Columbia V5A 1S6, Canada

Katherine Kelley

Graduate School of Oceanography, University of Rhode Island, Narragansett, Rhode Island 02882, USA

Adam J. R. Kent

College of Earth, Ocean and Atmospheric Sciences, Oregon State University, Corvallis, Oregon 97330, USA

Anthony E. Williams-Jones

Department of Earth and Planetary Sciences, McGill University, Montreal, Quebec H3A 0G4, Canada

[1] Subduction zone recycling of volatiles (H₂O, Cl, S, F) is controlled by the nature of subducted materials and the temperature-pressure profile of the downgoing slab. We investigate the variability in volatile and fluid-mobile trace element enrichment in the Sunda arc using melt inclusion data from Kawah Ijen and Tambora volcanoes, together with published data from Galunggung, Indonesia. Combining our results with data from other arcs, we investigate the mobility of these elements during slab dehydration and melting. We observe correlations between Sr, H₂O and Cl contents, indicating coupling of these elements during subduction zone recycling. Sulfur is more variable, and fluorine contents generally remain at background mantle values, suggesting decoupling of these elements from H₂O and Cl. Partial melting and dehydration models constrain the source of Sr and the volatiles and suggest that the altered oceanic crust (AOC) is the main source of the hydrous component that fluxes into the mantle wedge, in agreement with thermo-mechanical models. Sediment melt remains an important component for other elements such as Ba, Pb, Th and the LREE. The Indonesian volcanoes have variable concentrations of volatile and fluid-mobile elements, with Kawah Ijen recording higher AOC-derived fluid fluxes (Sr/Nd and H₂O/Nd) compared to Galunggung and Tambora. Kawah Ijen has H₂O/Ce ratios that are comparable to some of the most volatile-rich magmas from other cold slab subduction zones worldwide, and the highest yet measured in the Sunda arc.

Components: 15,500 words, 8 figures.

Keywords: H₂O-rich fluid; Sunda arc; fluid-mobile element; melt inclusion; subduction zone; volatile element.

Index Terms: 1031 Geochemistry: Subduction zone processes (3060, 3613, 8170, 8413); 1043 Geochemistry: Fluid and melt inclusion geochemistry; 1065 Geochemistry: Major and trace element geochemistry.

Received 18 April 2012; **Revised** 17 August 2012; **Accepted** 24 August 2012; **Published** 28 September 2012.

Vigouroux, N., P. J. Wallace, G. Williams-Jones, K. Kelley, A. J. R. Kent, and A. E. Williams-Jones (2012), The sources of volatile and fluid-mobile elements in the Sunda arc: A melt inclusion study from Kawah Ijen and Tambora volcanoes, Indonesia, *Geochem. Geophys. Geosyst.*, 13, Q09015, doi:10.1029/2012GC004192.

1. Introduction

[2] Recent geochemical and petrological studies have focused on obtaining a comprehensive data set of whole rock, glass and/or melt inclusion compositions in order to investigate the nature of the mantle wedge and the added subduction component involved in arc magma genesis [e.g., *Sisson and Bronto*, 1998; *Wysoczanski et al.*, 2006; *Churikova et al.*, 2007; *Portnyagin et al.*, 2007; *Sadofsky et al.*, 2008; *Johnson et al.*, 2009; *Rowe et al.*, 2009; *Auer et al.*, 2009; *Tollstrup et al.*, 2010; *Ruscitto et al.*, 2010]. The aim of these studies is to improve our understanding of the nature of subduction fluxes and how these correlate with the slab thermal regime. Recently, *Ruscitto et al.* [2012] compiled a global data set of arc melt inclusion volatile and trace element concentrations, along with associated slab thermal parameters, with the aim of relating the supply of subduction-derived components to volcano location within the arc and underlying slab thermal conditions. This compilation identifies systematic global trends, but more data are needed from end member subduction zones (very cold and very hot slabs) for a more complete understanding of subduction zone element recycling.

[3] This study contributes to the growing set of geochemical data for arc magmas, in particular from cold slab subduction zones, by providing melt inclusion compositional (major, trace and volatile) data from two volcanoes in Indonesia: Kawah Ijen volcano in eastern Java, which erupts H₂O-rich calc-alkaline magmas, and Tambora volcano on the island of Sumbawa, which erupts high-K magmas rich in incompatible elements but relatively poor in H₂O. Both volcanoes are located in the Sunda arc, which overlies one of the oldest and coldest subducting slabs in the world. The range of magma compositions erupted in the Sunda arc mirrors the global variability in subduction zone magmas, thus

making this region ideal for the study of subduction-related magmatic processes. The presence of coeval tholeiitic, calc-alkaline, shoshonitic and leucitic lavas suggests that a range of magma compositions can be produced within the same subduction system through interaction between mantle of different composition and fluids/melts from the slab [*Whitford et al.*, 1979; *Nicholls and Whitford*, 1983; *Wheller et al.*, 1987; *Turner and Foden*, 2001]. Both decompression melting and fluid-flux melting of the mantle have been proposed [*Nicholls and Whitford*, 1983; *Edwards et al.*, 1991], and the presence of low-H₂O magma at Galunggung volcano, located on the Sunda arc volcanic front, has contributed to the debate on the interplay between the two melting mechanisms in the production of arc magmas [e.g., *Sisson and Bronto*, 1998; *Kelley et al.*, 2006; *Kohut et al.*, 2006; *Vigouroux et al.*, 2008; *Reagan et al.*, 2010]. These observations highlight the importance of characterizing the exact nature of the mantle wedge, the melting mechanism and the added subduction component in the study of subduction zone element recycling.

[4] In this contribution, we compare new melt inclusion compositional data with existing data from Galunggung volcano in central Java, and interpret these in light of dehydration and melting models for the subducting slab beneath Indonesia, in order to gain insight into the nature of the subduction component involved at each volcano. We use experimentally determined trace element mobility data for subducting slabs [e.g., *Kessel et al.*, 2005; *Klimm et al.*, 2008, *Hermann and Rubatto*, 2009], information on the nature of the slab being subducted [e.g., *Plank and Langmuir*, 1998] and thermo-mechanical models of slab dehydration [e.g., *Rüpke et al.*, 2002, 2004; *Hacker*, 2008] to constrain these models. The same approach is used to compare the Indonesian volcanoes to other arc volcanoes worldwide (Mexico, Central America, Central Cascades, and Kamchatka) in an attempt to characterize the

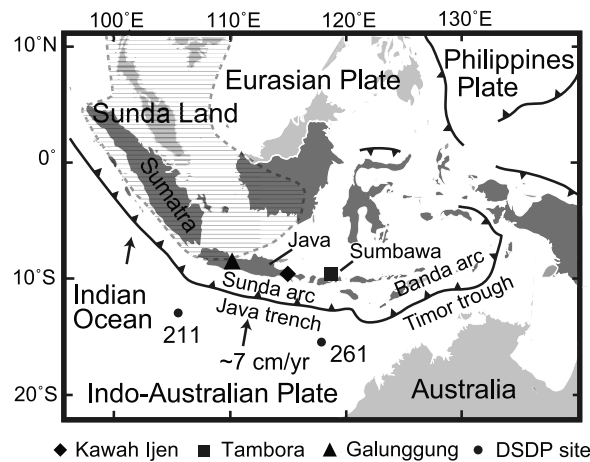


Figure 1. Map of the Sunda arc, Indonesia, showing the locations of Galunggung, Kawah Ijen and Tambora volcanoes. The thatched region labeled Sunda Land delineates the inferred extent of the continental lithosphere beneath the arc [Hamilton, 1979]. Arrows indicate relative plate motions [Tregoning et al., 1994] and convergence rate [Syracuse and Abers, 2006]. Also shown are drill core recovery sites from the Deep Sea Drilling Project (DSDP) as discussed in Plank and Langmuir [1998].

global variability and to investigate controls over volatile and trace element patterns at subduction zones. In particular, we aim to 1) investigate the correlation between the fluid-mobile trace elements and the volatiles, to establish the best non-volatile trace element proxy for the dehydration of the slab (e.g., Ba, Sr, Pb), and 2) investigate trace element ratios that may provide a means of discriminating between the subduction component reservoirs (altered oceanic crust or sediment) sourcing these volatiles.

2. Geologic Setting

[5] Kawah Ijen, Tambora and Galunggung are located along the volcanic front of the Sunda arc, a mixed continental/oceanic arc in Indonesia. The Sunda arc is related to the subduction of the Indo-Australian plate beneath the Eurasian plate along the 1200 km long Java trench (Figure 1). From west to east, Galunggung is located in western Java about 180 km from the capital city Jakarta, Kawah Ijen is found at the eastern tip of the island, ~700 km east of Galunggung, and Tambora is located ~400 km further east on the island of Sumbawa.

[6] In Sumatra and the western part of Java, the overriding plate is composed of continental crust

with continental lithospheric basement, part of the “Sunda Land” terrane [Hamilton, 1979]. Beneath Kawah Ijen, the crust is thinner and mainly composed of accreted Cretaceous oceanic and Archean continental terranes [Smyth et al., 2007; Clements et al., 2009]. Galunggung is located east of the inferred boundary of the continental basement and sits on Cretaceous ophiolites [Clements et al., 2009]. Further to the east, Tambora sits on oceanic crust of Miocene or younger age, composed mainly of volcanics, limestones and sandstones [Foden, 1986].

[7] The nature and age of the subducting plate varies along the arc from nearly orthogonal convergence of old oceanic crust (145 Ma) offshore of Tambora, to more oblique and transpressive subduction of younger oceanic crust (96 Ma) offshore of Galunggung [Hamilton, 1979; Tregoning et al., 1994; Syracuse and Abers, 2006]. Within the island of Java, the volcanic front as a whole moved ~50 km north away from the trench sometime after the Paleogene, which resulted in a pronounced increase in the arc front distance to the trench and depth to the top of the slab near Kawah Ijen (180 km versus 120 km depth for Galunggung) [Hamilton, 1979; Syracuse and Abers, 2006], and a broader distribution of the volcanic arc near Galunggung [Clements et al., 2009]. Tambora lies 150 km above the slab [Syracuse and Abers, 2006], just west of the transition between the Java trench and the Timor trough, the latter associated with the subduction of Australian continental material [Hamilton, 1979; Foden and Varne, 1980].

[8] The sediment package being subducted along the Java trench has been characterized in detail by Plank and Langmuir [1998]. An uppermost layer of siliceous ooze (125 m thick) overlies 45 m of sand/clay/silt turbidites, followed by 130 m of pelagic clay. This sediment column is an average for the Java trench determined from two Deep Sea Drilling Project (DSDP) drill sites located at the eastern and western ends of Java (Figure 1). The western end is characterized by the presence of turbidites originating from large off-shore fans transporting sediment from the Himalayan collision zone. The eastern sedimentary sequence contains carbonate-rich turbidites originating from the Australian continent. The thickness of the sedimentary package offshore of the Java trench is relatively uniform (200–400 m thick) but the amount of sediment in-fill at the trench varies laterally. Offshore of Galunggung, the accretionary margin contains up to 1 km of sediment in-fill,

whereas offshore of Kawaj Ijen and Tambora, sedimentary in-fill is nearly absent [Kopp *et al.*, 2006].

[9] Galunggung is a stratovolcano with a history of large explosive eruptions including a significant sector collapse around 4200 BP (^{14}C age) [Bronto, 1989] and eruption yielding large pyroclastic flows alternating with periods of dome growth. The latest explosive event was in 1982–83 and was characterized by the eruption of mafic material (basalt-andesite) including tephra deposits with ash to scoria size clasts [Sisson and Bronto, 1998; de Hoog *et al.*, 2001]. The samples discussed in this study are high-Mg basaltic bombs from the 1982–83 eruption and the melt inclusions have been analyzed by Sisson and Bronto [1998] and de Hoog *et al.* [2001]. These authors note the presence of two populations of melt inclusions, one characterized as a basaltic melt, the other as a silica-undersaturated, CaO-rich melt [Sisson and Bronto, 1998] (see further discussion below).

[10] Kawah Ijen is a small, active stratovolcano within the Ijen Caldera Complex. The volcanic edifice has been built and subsequently destroyed over the last 24,000 years [Sitorus, 1990; van Hinsberg, 2001], starting with a cone-building stage that consists of interbedded layers of basaltic scoria and lava flows. These are overlain by interbedded pyroclastic flow and fall deposits, phreatic deposits, and more felsic lava flows [Sitorus, 1990]. Samples of coarse ash to fine lapilli size scoria from the lowermost exposed layers of the edifice were collected in order to sample the earliest and most primitive magmas erupted at Kawah Ijen.

[11] Tambora volcano is a large, active stratovolcano on the volcanic front that is best known for its great explosive eruption in 1815, which is the largest volcanic eruption in modern history [Self *et al.*, 1984]. The samples used in this study are from the Black Sands formation, a 100-m thick deposit of dark grey to black sandy volcanic ash that bears abundant olivine phenocrysts. The Black Sands Formation was deposited following the initial caldera-forming eruption of Tambora ~43,000 years ago and it pre-dates the catastrophic 1815 eruption, although its exact age is unknown [Sigurdsson and Carey, 1992].

3. Samples and Methodology

[12] The melt inclusions from both Kawah Ijen and Tambora are glassy and reflect rapid quenching of the samples during explosive eruption. They range in size from 60–230 μm in maximum length, the

average being 100 μm in length, and their dominant shape is ellipsoidal. Many of the Kawah Ijen and Tambora melt inclusions contain a co-entrapped opaque crystal and most contained a small shrinkage vapor bubble. In the Kawah Ijen sample set, one melt-filled embayment was also analyzed (sample TO-IX). It is glassy despite being visibly connected to the groundmass.

[13] Melt inclusions from Kawah Ijen were analyzed using a combination of Fourier Transform Infrared Spectroscopy (FTIR) for the volatiles (H_2O , CO_2), electron microprobe for the major elements, S, Cl and F, as well as the S $\text{K}\alpha$ peak position (for oxygen fugacity determination), and Laser Ablation ICP-MS (LA ICP-MS) for the trace elements. Tambora melt inclusions were analyzed by ion microprobe for the volatile elements, electron microprobe for major elements, and LA ICP-MS for the trace elements. Details of the analytical procedures can be found in the auxiliary material (Text S1).¹

4. Results

[14] Melt inclusion compositions from Kawah Ijen and Tambora, along with calculated oxygen fugacities (for Kawah Ijen only), are reported in Table S1 in the auxiliary material. These compositions have been corrected for post-entrapment crystallization (see Text S1 in the auxiliary material for details). A summary of the Galunggung melt inclusion compositions is also presented in Table S1. Only values corrected for post-entrapment crystallization are described in the text and figures. Uncorrected compositions are presented in Table S2 of the auxiliary material for Kawah Ijen and Tambora and in Sisson and Bronto [1998] and de Hoog *et al.* [2001] for Galunggung.

[15] Olivine host compositions range from Fo 78 to 81 for Kawah Ijen and from Fo 67 to 72 for Tambora. In comparison, they range to more primitive values (Fo 78–89) for Galunggung [Sisson and Bronto, 1998; de Hoog *et al.*, 2001]. The Kawah Ijen basaltic melt inclusions (with the exception of a melt embayment from sample TO-IX) have anhydrous normalized SiO_2 values of 47–49 wt%, Al_2O_3 contents of 19–20 wt%, CaO contents of 11–12 wt% and MgO contents of 5–7 wt%, and can be classified as high-alumina basalt [Kuno, 1960]. Tambora magmas are basaltic trachyandesites and trachyandesites with 54–57 wt% SiO_2 , 2–3 wt%

¹Auxiliary materials are available in the HTML. doi:10.1029/2012GC004192.

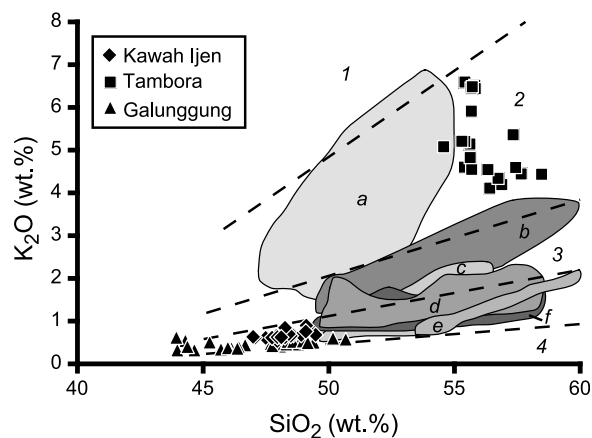


Figure 2. Major element composition, K_2O versus SiO_2 (wt%), of the Sunda arc magmas. Data for Kawah Ijen, Tambora and Galunggung (see Table S1) are olivine-hosted melt inclusion compositions calculated to be in equilibrium with their host olivine (and normalized on an anhydrous basis). Shaded fields represent whole rock data for other Sunda arc volcanoes (a = Muriah [Calanchi et al., 1983; Edwards et al., 1991], b = Merapi [Camus et al., 2000; Gertisser and Keller, 2003; Nadeau et al., 2010] (olivine-hosted, corrected, melt inclusion compositions), c = Tangkuban [Sendjaja et al., 2009], d = Slamet [Vukadinovic and Sutawidjaja, 1995; Reubi et al., 2003], e = Salak [Handley et al., 2008], f = Batur [Reubi and Nicholls, 2004]). Labeled fields delineated by the dashed lines are: 1 = Leucitite, 2 = Shoshonite, 3 = High-K calc-alkaline, and 4 = Low-K tholeiite. Classification scheme from Peccerillo and Taylor [1976].

MgO and 4–7 wt% K_2O . They likely represent the evolved product of parental trachybasalt after fractionation of olivine, clinopyroxene, plagioclase and magnetite [Foden, 1986]. In contrast, Galunggung magmas have higher and more variable MgO (6–11 wt%) and CaO (12–19 wt%) contents as well as variable SiO_2 contents (44–51 wt%), and the melt inclusions span a range of compositions between two end member primitive melts: a basalt, and a high-Ca, silica-undersaturated melt similar in composition to an ankaramite [Sisson and Bronto, 1998; de Hoog et al., 2001; Kelley et al., 2006]. Both types of inclusions were found in single olivine crystals [de Hoog et al., 2001] and are hosted in a high-Mg basalt. Sisson and Bronto [1998] relate the melt inclusions to the host high-Mg basalt by deep fractionation of olivine and diopsidic clinopyroxene with up to 25% mixing with a silica-undersaturated, high-Ca melt. The volatile data available from the Galunggung melt inclusions spans the entire range of major element compositions.

[16] Melt inclusion compositions from Kawah Ijen classify mostly as medium-K calc-alkaline magmas,

while Galunggung magmas straddle the boundary between low-K tholeiitic and medium-K calc-alkaline magmas and Tambora melt inclusions classify as shoshonites (Figure 2). For comparison, whole rock data for other volcanoes within the Sunda arc are shown. They illustrate the range of magma compositions that can erupt in close spatial and temporal proximity; all of the Indonesian volcanoes shown, including Kawah Ijen, Tambora and Galunggung, have had historical eruptions, except for Muriah, which was active in the Holocene [Siebert and Simkin, 2002].

[17] The trace element patterns of the Indonesian magmas are compared in Figure 3. On average, the compositions display the typical enrichment-depletion pattern of subduction zone magmas with a variable but distinct depletion in some of the high field-strength elements (HFSE) such as Nb (and Zr for Kawah Ijen and Galunggung). They also show a relative enrichment in Pb and the large ion lithophile elements (LILE) over the light rare earth elements (LREE) when compared to average normal mid-ocean ridge basalt (NMORB) and ocean island basalt (OIB) magmas (Figure 3a).

[18] Kawah Ijen and Galunggung display somewhat similar trace element patterns and similar absolute element concentrations. However, Galunggung magmas have a relatively flat REE pattern compared to Kawah Ijen (average $La/Yb = 2.5$ compared to 5.6 for Kawah Ijen; Figure 3b), and lower Sr concentrations relative to the LREE (e.g., average $Sr/Nd = 23$ compared to 45 for Kawah Ijen; Figure 3a). Tambora magmas lack a positive Sr anomaly and have a pronounced negative Ti anomaly and a steep REE pattern (average $La/Yb = 15$; Figure 3).

[19] In terms of volatile contents, the Kawah Ijen melt inclusions are notably different in comparison to Tambora and Galunggung (Figure 4). They display a wide range of H_2O and CO_2 contents, starting with water-rich compositions (~ 7 wt% H_2O at 1700 ppm CO_2). In contrast, Tambora melt inclusions have < 2 wt% H_2O and low CO_2 contents (< 250 ppm). Galunggung melt inclusions have low H_2O with variable CO_2 contents, up to 500 ppm [Sisson and Bronto, 1998].

[20] The vapor saturation isobars shown in Figure 4 indicate maximum melt inclusion trapping pressures of 400 MPa for Kawah Ijen, corresponding to depths of < 15 km in the crust, assuming the melts were vapor-saturated. The large range of H_2O and CO_2 contents recorded by the melt inclusions implies the melt was vapor saturated. The Tambora

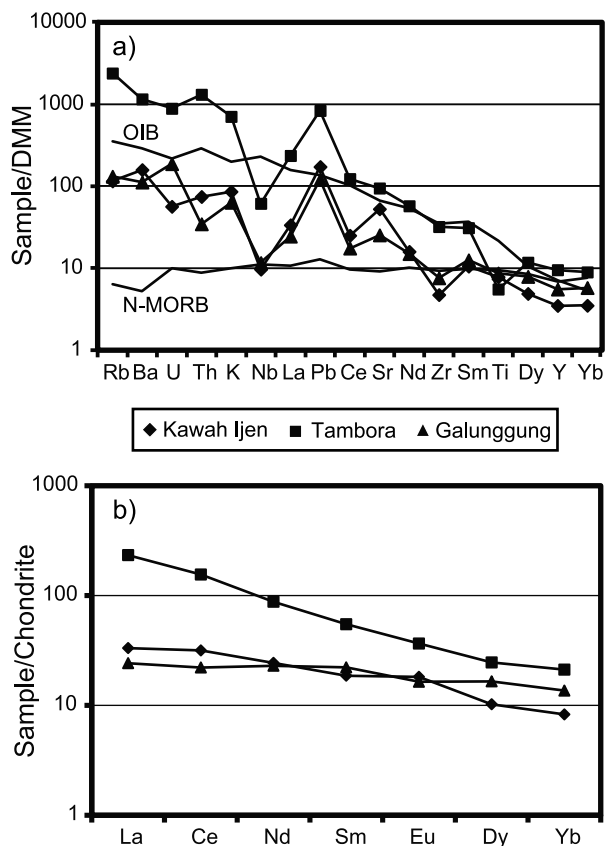


Figure 3. (a) Multi-element spider diagram normalized to depleted MORB mantle (DMM [Salters and Stracke, 2004]) and (b) REE diagram normalized to chondrite [Sun and McDonough, 1989]. Average values for melt inclusions from Kawah Ijen, Tambora, and Galunggung (Table S1) are shown together with data for average ocean island basalt (OIB) and normal MORB (N-MORB), both from Sun and McDonough [1989].

and Galunggung melt inclusions record relatively low saturation pressures (<100 MPa).

5. Discussion

5.1. Trace and Volatile Element Ratios

[21] In the following discussion, we compare the trace and volatile element signatures of the Indonesian volcanoes studied herein, and also examine global variability in volatile and trace element patterns at subduction zones by including published olivine-hosted melt inclusion data (compositions corrected to be in equilibrium with their olivine host) from other arc volcanoes (Mexico, Central America, Cascades, and Kamchatka; Table S3 in the auxiliary material).

[22] For comparison between the different arc magmas, we use element ratios in order to limit the effect of variable degrees of fractional crystallization among the different magmas. This approach assumes that no mineral crystallizing from these primitive mantle melts fractionates the selected trace (La, Ce, Sm, Nd, Dy, Yb, Nb, Y, Th, Sr, Ba) and volatile (H_2O , S, Cl, F) elements from each other and that no crustal assimilation of trace element- or volatile-enriched phases occurs. The data used for comparison in this study are derived mainly from primitive, olivine-hosted melt inclusions, with evidence for only minor olivine- and/or clinopyroxene-dominated fractionation from parental, mantle-derived magmas (e.g., Mexico: Johnson *et al.* [2009]; Galunggung:

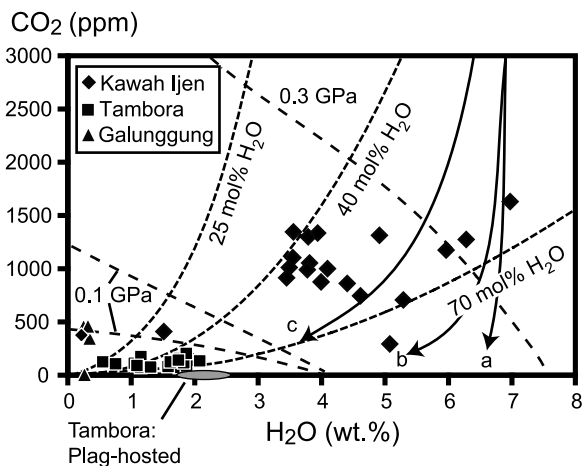


Figure 4. CO_2 versus H_2O contents of melt inclusions from Kawah Ijen, Tambora and Galunggung. Compositions are in equilibrium with their host olivine. The standard deviation for a given melt inclusion from duplicate analyses (when available) is generally smaller than the symbol size. The grey shaded field represents the range of H_2O contents determined by FTIR by Gertisser *et al.* [2012], on plagioclase-hosted melt inclusions from the 1815 eruption of Tambora (CO_2 contents were below detection limit). Widely dashed curves are isobars from Papale *et al.* [2006] calculated from the average composition and temperature of the melt inclusions. The lower isobar labeled 0.1 GPa is calculated for Tambora conditions, the 0.3 GPa isobar represents Kawah Ijen conditions only. Solid curves are calculated degassing paths for the Kawah Ijen melt inclusions (a = open system, b = closed and c = closed with 5 wt% exsolved vapor) and closely dashed curves are isopleths of constant vapor composition, calculated using VolatileCalc [Newman and Lowenstern, 2002]. The starting melt composition was chosen to have the highest H_2O found in the Kawah Ijen melt inclusions with a total of 6000 ppm CO_2 based on the assumption that there has been >50% CO_2 degassed by 0.3 GPa [Wallace, 2005; Blundy *et al.*, 2010].

de Hoog et al. [2001]). For some of the more evolved melt inclusions, including Kawah Ijen [Handley et al., 2007], Tambora [Foden, 1986], Kamchatka [Portnyagin et al., 2007] and Central America [Sadofsky et al., 2008], additional fractionation of Fe-oxides and plagioclase is likely. Apart from plagioclase fractionation, which will affect ratios involving Sr, these crystallizing assemblages should have minimal effect on the ratios we used. As discussed in more detail below, the lack of a global correlation between indices of differentiation and average Sr/Nd ratio, as well as significant correlations between Sr/Nd and volatile element ratios (e.g., H₂O/Ce), suggests that any effect of plagioclase fractionation on the Sr/Nd ratio of a particular magma is small compared to the global variation in Sr/Nd ratios as a result of subduction component addition.

[23] Kawah Ijen basaltic magmas show evidence of minor Cl-rich apatite fractionation [Vigouroux, 2011] and therefore ratios involving Cl should be considered minimum values. Some of the magmas examined in this study may also have fractionated a sulfur-rich phase (e.g., immiscible sulfide liquid), even if this phase is not easily preserved in erupted products. This has been documented in most magmas of Central America [Sadofsky et al., 2008], the Galunggung magmas [Sisson and Bronto, 1998], and may have been present in the Kawah Ijen magmas (K. Berlo et al., The provenance of metals in volcanic gases from Kawah Ijen volcano, Indonesia, submitted to *Chemical Geology*, 2012). Therefore, ratios involving S should also be interpreted with caution.

[24] The trace element ratios for each volcano still display some variability, which may be related to magma mixing (e.g., Galunggung), or simply variability in the primitive mantle melt composition due to mantle source heterogeneity and/or variability in the type and amount of subduction-derived fluid addition to the mantle source. Ideally, we would compare individual volcanoes based on the average of the trace element ratios for each melt inclusion suite. However, not all melt inclusions have a complete trace element analysis. Therefore, we calculate ratios based on the average concentration of each trace element from the melt inclusion suite and report the standard deviation for that suite.

[25] For ratios involving volatile components, we use only the highest H₂O values and the S, Cl and F contents associated with these maximum H₂O contents, thereby minimizing the effects of degassing. For most of the olivine-hosted melt inclusions

compared in this study, maximum H₂O and CO₂ contents correspond to saturation pressures ≥ 300 MPa and are likely representative of the primary (undegassed) or near-primary H₂O contents of these arc basalts, as confirmed, in some cases, with independent estimates based on experimental phase equilibria (e.g., Mexico) [Weaver et al., 2011].

[26] The H₂O and CO₂ contents of the Kawah Ijen melt inclusions are highly variable (from over 7 wt% to less than 1 wt%), which is characteristic of degassing magma during ascent and crystallization. However, the high CO₂ contents maintained even at low H₂O contents do not correspond to predicted degassing paths for basaltic magmas (Figure 4). These variable and high CO₂/H₂O ratios may be explained by gas fluxing from deeper in the conduit followed by partial re-equilibration with the magma upon ascent and degassing [e.g., Wallace, 2005; Spilliaert et al., 2006; Johnson et al., 2008; Vigouroux et al., 2008; Roberge et al., 2009; Blundy et al., 2010]. Conversely, any prolonged storage of the magma prior to eruption or slow cooling during eruption may have resulted in variable H loss from the melt inclusion due to rapid, post-entrapment diffusion [e.g., Portnyagin et al., 2008; Chen et al., 2011]. At Kawah Ijen, the prevalence of melt inclusions trapped at ~ 0.2 GPa suggests that stalling/storage of magma may have occurred at this lithostatic pressure, perhaps favoring variable re-equilibration of the melt with a CO₂-rich gas phase or H loss by diffusion. However, there is no observed correlation between the H₂O content (or H₂O/K₂O ratio) and the degree of post-entrapment crystallization in the melt inclusions. Given the possibility that H loss via diffusion occurs faster than post-entrapment crystallization, we cannot rule the process out.

[27] The degassed nature of the Tambora melt inclusions is reflected in the relatively low H₂O and CO₂ contents and vapor saturation pressures, therefore ratios involving the volatiles should be considered a minimum. Similar H₂O contents (1.8–2.5 wt%; CO₂ contents below detection limit) were found in more evolved (55–59 wt% SiO₂) plagioclase-hosted melt inclusions from the 1815 eruption [Gertisser et al., 2012]. Compared to Kawah Ijen, the pattern of H₂O and CO₂ concentrations of the Tambora melt inclusions are more typical of equilibrium degassing processes.

[28] The Galunggung magmas have variable CO₂ concentrations over a restricted range of low H₂O concentrations suggesting the magma was vapor saturated and lost variable amounts of CO₂ before

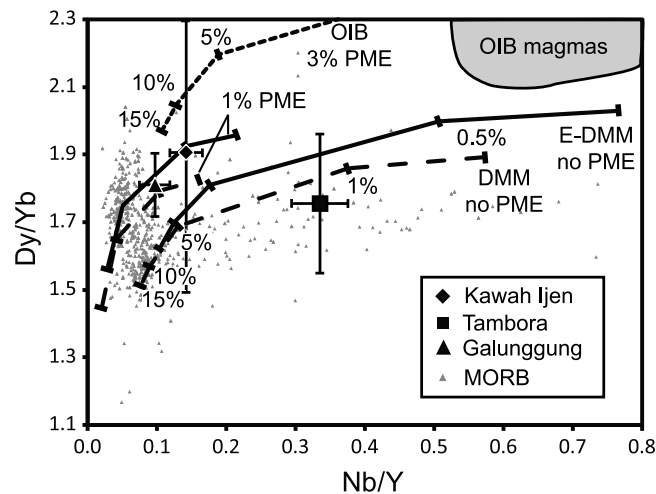


Figure 5. Dy/Yb versus Nb/Y of average melt inclusion compositions from Kawah Ijen, Tambora and Galunggung compared with MORB and OIB-type magmas. Error bars represent the standard deviation for each melt inclusion suite. MORB data is a compilation of mafic volcanics from spreading centers compiled from PetDB (<http://www.petdb.org>) [Lehnert et al., 2000]. OIB data is a compilation from Fernandina, Loihi and Piton de la Fournaise mafic volcanics [Geist et al., 2006; Dixon and Clague, 2001; Vlastélic et al., 2007]. The curves represent modal batch melting of a depleted MORB mantle (DMM from *Salters and Stracke* [2004]; dashed lines), and enriched DMM (E-DMM from *Workman and Hart* [2005]; solid lines) and an OIB-like mantle (from *Johnson et al.* [2009]; dotted line) in the spinel stability field (percent partial melting increments are the same for all curves). The mantle source has either undergone no episode of previous melt extraction (PME) or 1% PME in the spinel lherzolite stability field. See text for details of the modeling.

entrapment, but that H₂O contents are representative of the primary (undegassed) H₂O contents of these magmas [Sisson and Bronto, 1998]. The low-H₂O Galunggung melt inclusions have been ascribed to decompression melting of relatively dry, yet metasomatized mantle, which would explain the low H₂O contents despite the trace element pattern typical of subduction zones magmas [Sisson and Bronto, 1998; Schiano et al., 2000] (Figure 3a). However, given the evidence for fluid-enrichment in the mantle source of these magmas (Figure 3a), we do not discount the possibility that these melt inclusions were trapped with initially higher H₂O contents and were affected by post-entrapment loss of H via diffusion.

5.2. Mantle Source Composition

[29] To evaluate the contribution of the subduction component added to the mantle source beneath the Sunda arc, it is necessary to identify the nature of the mantle wedge prior to the addition of the subduction component. Some of the most conservative trace elements in subduction zones are the HFSE and the heavy REE [Pearce and Peate, 1995] because they are the least mobile during slab dehydration and melting [e.g., Kessel et al., 2005; Klimm et al.,

2008; Hermann and Rubatto, 2009]. We use these to characterize the nature of the mantle wedge and the degree of partial melting and previous melt extraction experienced by the mantle [e.g., Portnyagin et al., 2007; Johnson et al., 2009].

[30] Figure 5 compares the average melt inclusion Nb/Y and Dy/Yb ratios of the Indonesian volcanoes with modal batch melting models for various mantle source compositions in the spinel lherzolite stability field. Based on the partition coefficient data from *Workman and Hart* [2005], the Nb/Y ratio is a strong function of the degree of partial melting and episodes of previous melt extraction. The ratio is also sensitive, but to a lesser extent, to the mantle source composition. The Dy/Yb ratio is most affected by variations in mantle source composition. Elevated Dy/Yb ratios may reflect the presence of a OIB-like component in the mantle source of the arc magmas [e.g., Johnson et al., 2009].

[31] The Indonesian arc magmas have average Nb/Y and Dy/Yb ratios similar to MORB values, with Tambora falling within the range of enriched MORB values (higher Nb/Y) and Galunggung and Kawah Ijen plotting amongst normal MORB values. Mantle melting curves are modeled using the modal batch

melting equation and starting mantle compositions of depleted MORB Mantle (DMM [Salters and Stracke, 2004]), enriched DMM (E-DMM [Workman and Hart, 2005]) and an OIB-like mantle source from the Mexican arc [Johnson *et al.*, 2009]. Bulk partition coefficient (D) values used for modeling melting in the spinel stability field are from Workman and Hart [2005]. Following the method of Portnyagin *et al.* [2007], we also show model curves for partial melting of these mantle compositions after having undergone PME in the spinel stability field.

[32] These models do not offer a unique solution to the nature of the mantle source beneath these arc volcanoes. Variability among subduction zone magmas in terms of the fluid-immobile HFSE and HREE is likely a combined function of mantle wedge composition, degree of partial melting and degree and nature of PME. The models are also highly sensitive to the D values employed. Nevertheless, a first-order approximation of the mantle source of arc magmas may be assessed (Figure 5). The low Nb/Y ratios of Kawah Ijen and Galunggung suggest either very large degrees of partial melting or derivation from a previously depleted (having undergone PME) mantle source. The highly variable Dy/Yb ratio of the Kawah Ijen magma (over a restricted range of Nb/Y) may be the result of melting from a heterogeneous mantle source (mixture of MORB-like and OIB-like domains). The slightly lower Nb/Y and Dy/Yb ratios of the Galunggung magmas and the smaller variability in the Dy/Yb ratio is consistent with somewhat larger degrees of partial melting or PME of a more homogenous MORB-like mantle source. A MORB-like mantle source component (similar to Indian Ocean MORB; I-MORB) has previously been proposed for some of the magmas of Java [Turner and Foden, 2001; Gertisser and Keller, 2003; Sendjaja *et al.*, 2009] and Handley *et al.* [2007] identified an enriched I-MORB component in the magmas of Kawah Ijen using Sr, Nd, Hf and O isotopes. Some isotopic studies have found evidence for an OIB mantle component in the magmas of Java [e.g., Edwards *et al.*, 1991, 1994]. Therefore, we do not rule out the possibility of a mantle source containing a mixture of more enriched (OIB-like) and highly depleted mantle components (DMM). Tabora magmas plot close to the model curves for low degrees of partial melting of an E-DMM or DMM source without an episode of previous melt extraction. This is consistent with the geochemical modeling of Gertisser *et al.* [2012] who estimated ~2% partial melting of a garnet-free I-MORB-like mantle source for these magmas.

5.3. Sediment and Crustal Contributions to Arc Magmas

5.3.1. Source of Moderately Mobile Elements

[33] Although the more conservative elements such as the HFSE and HREE are used to model the mantle source beneath volcanic arcs, the more mobile elements such as the LILE, and moderately mobile elements such as the LREE and the actinides (U, Th) are influenced by the addition of hydrous melts from sediment and fluids from the altered ocean crust (AOC) [e.g., Hermann *et al.*, 2006; Kessel *et al.*, 2005; Klimm *et al.*, 2008; Hermann and Rubatto, 2009].

[34] Thorium and La are both moderately mobile elements during subduction zone recycling, especially at temperatures ≥ 900 °C and pressures ≥ 4 GPa, even if allanite and monazite are residual in the slab, and the two elements are not significantly fractionated from each other during slab dehydration and melting [Plank, 2005; Kessel *et al.*, 2005; Klimm *et al.*, 2008; Hermann and Rubatto, 2009]. The Th/La ratio is commonly used to track the addition of sediment melt to arc magmas because subducted sediment generally has a higher Th/La ratio compared to MORB and OIB mantle sources, and therefore sediment melt addition leads to elevated Th/La ratios in arc magmas [Plank, 2005; Plank and Langmuir, 1998].

[35] The contrasting Th/La ratios of sediment melt and AOC-derived fluid are illustrated in Figure 6a. The Th/La ratio of sediment melt was calculated using the partitioning data from the experiments of Hermann and Rubatto [2009] and the composition of subducted sediment averaged worldwide (GLOSS [Plank and Langmuir, 1998]), at temperature/pressure conditions likely occurring in the slab at sub-arc depths (800–1000 °C, 3.5–4.5 GPa). We note that the range in Th/La calculated for GLOSS (0.2–0.3) mirrors the range calculated for individual arcs (Java: 0.2–0.3; Mexico: 0.18–0.24; Kamchatka: 0.14–0.19; Cascades: 0.28–0.36) except for Central America (0.05–0.07) where the sediment being subducted has very low Th/La (0.06 [Plank and Langmuir, 1998]). Similarly, the Th/La ratio of fluids derived from the AOC was computed from the average of two AOC compositions reported by Kelley *et al.* [2003] and Bach *et al.* [2003] for two very different DSDP/ODP localities (offshore of the Mariana arc and the northern South American arc, respectively) and solid-fluid partition coefficient data for subducted oceanic basalt at 700–800 °C and

4 GPa from *Kessel et al.* [2005]. Fluids derived from the AOC have lower Th/La ratios compared to sediment melts. This reflects the slightly higher mobility of La over Th in lower temperature (700–800 °C) AOC-derived fluids [*Kessel et al.*, 2005] and the low Th/La content of average AOC compared to subducted sediment [*Plank and Langmuir*, 1998; *Kelley et al.*, 2003; *Bach et al.*, 2003].

[36] MORB magmas are unaffected by subduction-derived components and can serve as a good baseline for estimating the amount of sediment melt addition to arc magmas [e.g., *Plank*, 2005] (Figure 6a). However, episodes of previous melt extraction (PME) in the mantle source of arc magmas can lead to Th/La ratios lower than MORB values [*Portnyagin et al.*, 2007; *Johnson et al.*, 2009]. Therefore, we calculated the composition of hypothetical “dry mantle melts” produced by melting of the previously-depleted mantle beneath Kamchatka [*Portnyagin et al.*,

2007] and Mexico (excluding San Juan) [*Johnson et al.*, 2009] assuming 1–10% modal batch melting in the spinel stability field with D values from *Workman and Hart* [2005]. The resulting Th/La ratios of <0.08 are a more accurate baseline for the evaluation of sediment melt addition to arc magmas than the compositions of MORB alone (Figure 6a).

[37] Kawah Ijen, Tambora and Galunggung magmas have Th/La ratios that are significantly elevated above our “dry mantle melts” composition, and above AOC-derived fluid compositions, suggesting the addition of some sediment-derived melt, particularly for Tambora and Galunggung. For comparison with the Indonesian arc magmas, we compiled average olivine-hosted melt inclusion trace element and maximum H₂O contents from arc volcanoes worldwide (Mexico: *Johnson et al.* [2009]; Central America: *Wade et al.* [2006]; *Benjamin et al.* [2007]; *Sadofsky et al.* [2008]; the Central High Cascades: *Ruscitto et al.* [2010]; and Kamchatka: *Portnyagin et al.* [2007]; *Auer et al.* [2009]). As expected, most arc magmas show elevated Th/La ratios compared to the computed “dry mantle melts”, consistent with the importance of sediment-derived components on the overall slab flux [*Plank*, 2005].

5.3.2. Slab Surface Temperatures

[38] The temperature dependence of trace element mobility in subducting slabs, using the method of

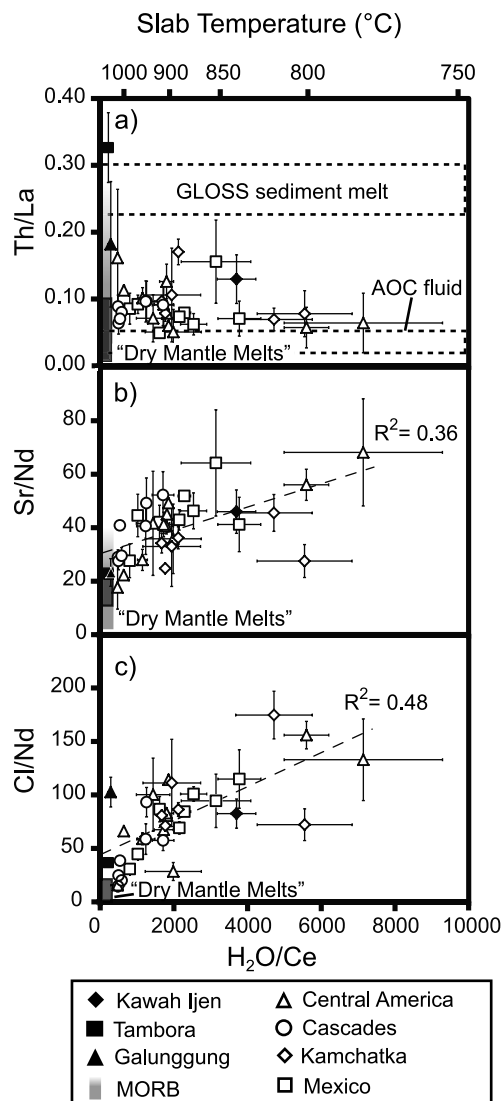


Figure 6. (a) Th/La, (b) Sr/Nd and (c) Cl/Nd versus H₂O/Ce of arc magmas. Thick dashed boxes in Figure 6a represent the Th/La ratio of sediment melt (bulk global subducted sediment: GLOSS [*Plank and Langmuir*, 1998]) at temperatures 800–1000 °C and the Th/La ratios in an AOC-derived fluid at 700–800 °C (using bulk AOC from *Bach et al.* [2003] and *Kelley et al.* [2003]). Modeling procedures are described in the text. The dark shaded bar labeled “Dry Mantle Melts” represents 1–10% partial melts of arc mantle sources after PME, and without the addition of a subduction component (Kamchatka [*Portnyagin et al.*, 2007]; Mexico [*Johnson et al.*, 2009]; see text for details). The gradationally shaded bar in Figures 6a and 6b represents global mafic MORB volcanics compiled from PetDB (<http://www.petdb.org>) [*Lehnert et al.*, 2000] with the shading proportional to the number of samples. Slab surface temperatures are calculated from the H₂O/Ce ratio of the melt inclusions using the method of *Plank et al.* [2009]. Error bars are calculated from the standard deviation of average Th, La, Ce, Nd and Sr contents at a given volcano, propagated through the ratio operation. Linear regression lines (thin dashed lines) and correlation coefficients are given in Figures 6b and 6c.

Plank et al. [2009], is also explored (Figure 6). This geothermometer utilizes the temperature dependence of Ce solubility in monazite- and allanite-saturated fluids/melts and the H₂O contents measured in experiments of high-pressure fluids/melts from sediment and oceanic basalt at a variety of temperatures [*Plank et al.*, 2009, and references therein]. It is important to note that there are several assumptions and uncertainties associated with this geothermometer [see *Plank et al.*, 2009], and as a result we simply use these estimated temperatures to investigate the possible relationship between slab temperature and trace element mobility.

[39] Melt inclusion H₂O/Ce ratios, using maximum (least degassed) H₂O contents, are ~3700 for Kawah Ijen, ~220 for Tambora and ~285 for Galunggung, reflecting the elevated H₂O content of the Kawah Ijen magmas (Figure 6). The corresponding slab surface temperature is ~800 °C for Kawah Ijen. The H₂O/Ce ratios of the Tambora and Galunggung magmas are similar to those of average MORB [*Saal et al.*, 2002] and only slightly above values calculated for “dry mantle melts”, which would suggest a minimal slab-derived H₂O-rich fluid component in these magmas and elevated slab surface temperatures of 1050 and 1025 °C, respectively. However, as discussed earlier, partial degassing of H₂O from the Tambora magma prior to melt inclusion formation results in an underestimate of the H₂O/Ce ratio.

[40] In the calculation of slab surface temperatures, it is more accurate to employ the H₂O/Ce ratio of the subduction component as opposed to the melt composition because the mantle wedge may contribute significant amounts of Ce, thereby imparting a lower H₂O/Ce ratio to the magma [*Ruscitto et al.*, 2012]. However, there are a number of assumptions and uncertainties involved in calculating the subduction component of arc magmas [see *Portnyagin et al.*, 2007]. A comparison of temperature estimates using both the calculated subduction component from *Portnyagin et al.* [2007] and *Johnson et al.* [2009] and the measured H₂O/Ce ratio in the melt inclusions suggests that slab surface temperatures may be overestimated by up to 60 °C when using the latter.

[41] There is no obvious correlation between slab surface temperatures and Th/La ratio (Figure 6a). This agrees with experimental studies that have shown that Th/La ratios in allanite- and monazite-saturated sediment [*Hermann and Rubatto*, 2009] and AOC-derived [*Kessel et al.*, 2005; *Klimm et al.*,

2008] fluids/melts do not vary significantly as a function of temperature or degree of melting. Therefore, the variability is a result of variable proportions of sediment melt added to the mantle source of the arc magmas. However, we note that there is a tendency for magmas with the lowest H₂O/Ce ratios to have the highest Th/La ratios, and therefore higher proportions of sediment melt, consistent with the results of *Ruscitto et al.* [2012].

[42] In contrast, there is an inverse correlation between slab temperature and Sr/Nd and Cl/Nd ratios (Figure 6b, $r^2 = 0.36$; and 6c, $r^2 = 0.48$, both significant at the 95% confidence level). In contrast to Th and La, Sr and Cl are both highly fluid-mobile elements, and Nd behaves similarly to La and Ce (moderately mobile at temperatures ≥ 800 °C and pressures ≥ 4 GPa [*Kessel et al.*, 2005; *Hermann and Rubatto*, 2009]). The inverse correlation of Sr/Nd with slab temperature is consistent with experimental results on sediment and AOC dehydration/melting in which Sr is highly mobile at low temperatures and low fluid/melt fractions compared to the LREE, and Sr/Nd ratios decrease as temperature increases [*Green and Adam*, 2003; *Kessel et al.*, 2005; *Klimm et al.*, 2008; *Hermann and Rubatto*, 2009].

[43] A correlation between Sr/Nd and H₂O/Ce may also exist irrespective of any temperature-dependent devolatilization processes within the slab because plagioclase fractionation in primitive mantle-derived melts with low H₂O contents, and conversely the suppression of plagioclase crystallization in hydrous basaltic melts, could impart this correlation. However, we note that within the range of compositions sampled by the melt inclusions (olivine host forsterite contents range from 72–91), there is no correlation between the extent of differentiation by fractional crystallization and the H₂O/Ce or Sr/Nd ratios for data from Fo ≥ 80 olivine (over 80% of the data). Inclusions hosted in Fo 90–91 olivine, where plagioclase is unlikely to be a liquidus phase, show almost the full range of H₂O/Ce and Sr/Nd ratios. For the more evolved melt compositions (olivine Fo 72–79; <20% of the data), including Tambora, there is a correlation ($r^2 = 0.61$, significant at 90%), however, the range of H₂O/Ce and Sr/Nd exhibited by these more evolved melts also overlaps with the range found in the most primitive olivine (Fo 90–91). From this we conclude that the correlation between H₂O/Ce and Sr/Nd is not dominantly controlled by the presence or absence of plagioclase on the liquidus of these melts during olivine-hosted melt inclusion

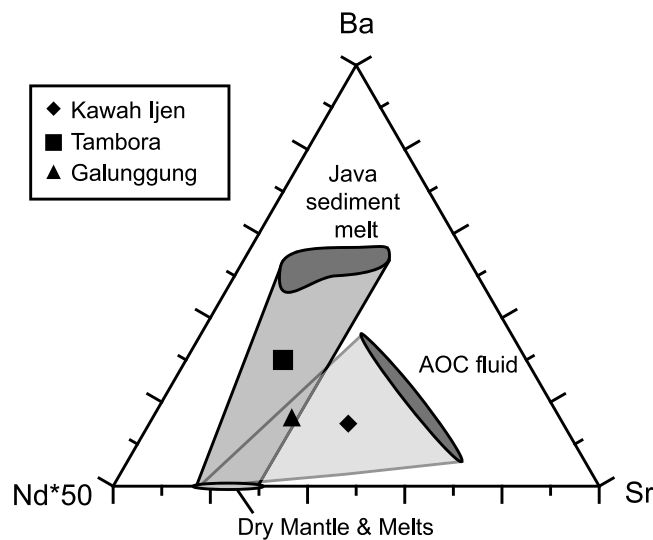


Figure 7. Sr-Nd-Ba ternary diagram illustrating the role of the two main subduction components: sediment melt and AOC-derived fluids, calculated at temperatures of 750–1000 °C. Details of the fluid/melt composition modeling are described in the text. Field labeled “Dry Mantle & Melts” encompasses both the mantle source of arc magmas prior to subduction zone enrichment (from *Portnyagin et al.* [2007] and *Johnson et al.* [2009]) and 1–10% partial melts from these mantle sources.

trapping, but is related to variable amounts of addition of a subduction-derived component.

[44] Chlorine is also highly mobile as evidenced by its correlation with H₂O contents in arc magmas [*Kent et al.*, 2002; *Johnson et al.*, 2009; *Ruscitto et al.*, 2012] and from high salinities in subduction zone metamorphic fluids [*Philippot et al.*, 1998; *Scambelluri et al.*, 2004]. The similar behavior of Sr and Cl with changing slab temperature suggests that, like Sr, Cl mobility is highest at low temperatures and/or low fluid/melt fractions.

5.3.3. Source of Fluid-Mobile Elements and Volatiles

5.3.3.1. Fluid-Mobile Elements

[45] The most mobile trace elements during slab subduction are the LILE (Cs, Rb, Ba, Sr) as well as Pb, B, Be and Li [*Kessel et al.*, 2005; *Marschall et al.*, 2007; *Klimm et al.*, 2008; *Hermann and Rubatto*, 2009]. In melt inclusion studies, these elements are not all routinely analyzed due to low concentrations. Some of the most commonly and most accurately analyzed elements are Sr and Ba because they occur in high concentrations (100s of

ppm). We have used Ba/Nd and Sr/Nd ratios to constrain the source of these fluid-mobile elements because sediment melt and AOC-derived fluids have very distinct compositions in Ba-Sr-Nd space (Figure 7).

[46] The sediment melt composition for the Java arc was calculated using the same method as described above (Figure 6a). The sediment melt field has variable Sr/Nd ratios that correspond to temperature variations from 750–1000 °C; pressure has only a negligible effect on the Sr/Nd ratio of the melt [*Hermann and Rubatto*, 2009]. The variation in Ba/Sr ratio is attributed to temperature, pressure and melt fraction variations [*Hermann and Rubatto*, 2009].

[47] The compositions of AOC-derived fluids were also calculated as described above. The fluids have higher average Sr/Nd and Sr/Ba ratios but lower Ba/Nd ratios compared to sediment melt (Figure 7). This mainly reflects the difference in composition of subducted sediments and AOC, despite the fact that Ba is slightly more mobile than Sr in AOC-derived fluids [*Kessel et al.*, 2005; *Hermann and Rubatto*, 2009]. Although not shown, the calculated composition of sediment melt from all the arcs discussed in this study, regardless of temperature, has elevated Ba/Sr compared to AOC-derived fluids, with the exception of Central America because the Ba/Sr ratio of these sediments is particularly low [*Plank and Langmuir*, 1998]. This makes the Ba/Sr ratio a good indicator of the nature of the subduction-derived component.

[48] Kawah Ijen, Galunggung and Tambora magmas have distinctly different Sr/Ba ratios with Kawah Ijen magmas being richer in Sr (and H₂O) compared to the other two. This is consistent with a greater proportion of AOC-derived fluid component for Kawah Ijen. In comparison, Tambora magmas fall within the field defined by mixing between a dry, depleted mantle source and sediment melt, consistent with the magmas’ elevated Th/La ratio. Galunggung magmas may contain contributions from both AOC-derived fluid and sediment melt because it plots in the intersection of these two fields (Figure 7).

[49] Isotopic studies have suggested an important role for AOC-derived fluids in all the magmas of the Sunda arc, including Galunggung, with, on average, a smaller proportion of a sediment-derived component [*Edwards et al.*, 1993; *Alves et al.*, 1999; *Turner and Foden*, 2001]. *Handley et al.* [2007] conducted a detailed trace element and isotope study of the lavas of the Ijen Caldera Complex. They suggested that a fertile MORB-like mantle

source was first fluxed with 3% AOC-derived fluid followed by the addition of <1% of bulk sediment. Interestingly, *Gertisser et al.* [2012] estimated a similar proportion of both components in the Tambora magmas (3% AOC-derived fluid and <1% sediment melt) from isotopic modeling, although they caution that the addition of AOC-derived fluid is not absolutely required by the model. We favor a smaller influence from AOC-derived fluids and a larger influence from sediment melt at Tambora based mainly on the low Sr/Nd and Sr/Ba ratios exhibited (Figure 7), as well as the elevated Th/La ratio (Figure 6a).

5.3.3.2. Volatile Elements

[50] Information on the mobility and partitioning of the volatile elements other than H₂O during slab dehydration and melting is scarce. In order to relate the volatile elements (H₂O, Cl, S and F) to their subduction component source, we considered their relationship with Sr, all ratioed to Nd (Figure 8). Using our compilation of melt inclusion data from arcs worldwide, we observed that Sr/Nd ratios are broadly correlated to H₂O/Nd ratios ($r^2 = 0.45$; 0.63 if the H₂O-rich yet Sr-poor magma of Kluckevskoy is omitted) and to a lesser extent Cl/Nd ratios ($r^2 = 0.33$) and S/Nd ratios ($r^2 = 0.23$), although all correlations are significant at the 95% confidence level. Fluorine contents do not appear to correlate with Sr contents and remain mostly near background mantle values. A correlation between the most fluid-mobile elements (H₂O, Sr, Cl) suggests that they are coupled during transfer from the slab to the mantle, whereas a poor or lack of correlation (S and F) suggests independent processes may control the concentration of these elements in subduction zone magmas.

[51] The global correlation between the volatiles and other fluid-mobile elements such as Pb and Ba needs to be examined on the scale of individual arcs because trends within individual arcs do not always mirror the global arc trend (see Figure S1 in the auxiliary material). Lead is highly mobile during both dehydration and melting of the AOC and sediment in the slab [*Tenthorey and Hermann, 2004; Kelley et al., 2005; Kessel et al., 2005; Hermann and Rubatto, 2009*] and its concentration correlates roughly with H₂O and Cl globally (Figure S1) but to a lesser degree than Sr (Pb/Ce versus H₂O/Ce and Cl/Ce: $r^2 = 0.19$ and 0.38, respectively).

[52] The correlation of Ba/La with H₂O/La ($r^2 = 0.14$) and Cl/La ($r^2 = 0.14$) is generally poor (Figure S1); Ba/La ratios for the Indonesian, Mexican and some

Kamchatka magmas are nearly constant over a range of H₂O/La ratios. In contrast, Central American magmas have a very wide range of Ba/La ratios for a more limited range in H₂O/La. We note that the stronger correlations found between H₂O/Ce, Ba/La and Cl/Nb by *Ruscitto et al.* [2012] resulted from inclusion of data from Tonga, which defines a global end member.

[53] The contribution of sediment melt to the total flux of trace elements such as Ba, Pb, Th and the LREE in arc magmas is undisputed [e.g., *Plank, 2005; Plank and Langmuir, 1993; 1998*] and stems from the combination of elevated concentrations of these elements in subducted sediment, as well as the enhanced mobility of these elements under most pressure-temperature conditions found in the top of the slab at sub-arc depths [e.g., *Hermann and Rubatto, 2009*]. However, the more complicated patterns observed for Ba/La, H₂O/La and Cl/La shown here suggest that in some arcs, Ba may be decoupled from H₂O and Cl. In contrast to Sr, the flux of Ba is mainly derived from the sediment layer, not the AOC, and the behavior of Ba during sediment melting is more complex compared to Sr. The concentration of Ba in fluids or melts varies with temperature, pressure, and degree of melting [*Kessel et al., 2005; Klimm et al., 2008; Hermann and Rubatto, 2009*], and residual phengite in the slab sediment may play a role in buffering Ba concentrations [*Hermann and Rubatto, 2009*]. Conversely, no residual phases retain Sr in the slab at sub-arc depths and temperatures ≥ 700 °C [*Feineman et al., 2007; Schmidt and Poli, 1998*]. Its concentration in the fluid or melt phase is governed in large part by the fraction of fluid/melt produced, which in turn is a function of temperature [*Hermann and Rubatto, 2009*]. As such, the ratio of Sr to a less mobile element (such as Nd) in arc magmas can act as a proxy for both the amount of AOC-derived aqueous fluid added to a given mantle source and the temperature of the slab at sub-arc depths.

[54] *Mobility of H₂O.* For the majority of the arc basalts, H₂O and Sr contents are variably elevated above background mantle values (the H₂O/Nd and Sr/Nd ratios of a dry, depleted mantle source are similar to MORB/OIB values), and their positive correlation implies that they are mostly coupled during slab dehydration and mantle melting at sub-arc depths.

[55] The proportion of total subduction-derived fluid in the various arc magmas can be assessed from the H₂O/Nd and Sr/Nd ratios of the magmas.

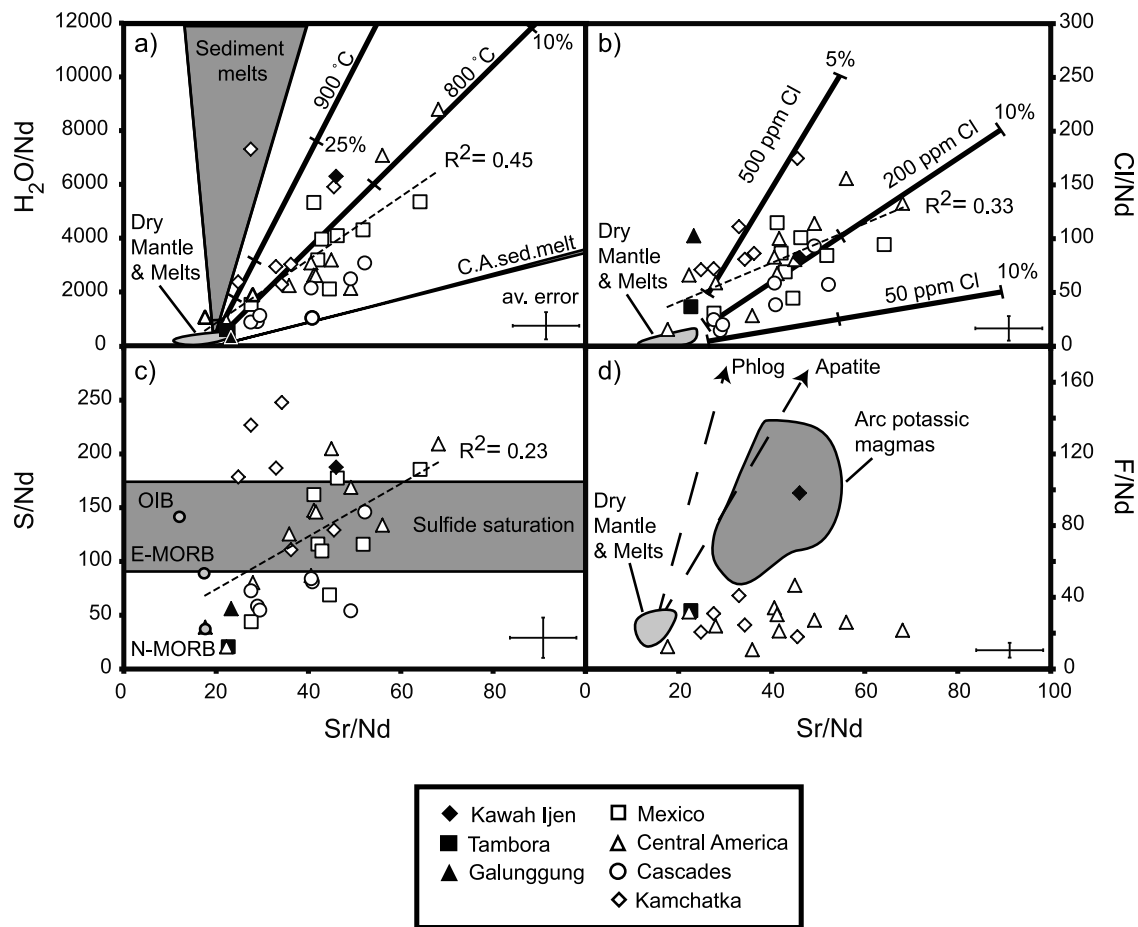


Figure 8. Variations in volatile content (a) H₂O; (b) Cl; (c) S and (d) F of subduction zone magmas with respect to Sr (all normalized to Nd). Average error bars are calculated as in Figure 6. Data sources and symbols are the same as in Figure 6, except for MORB and OIB values in Figure 8c. Field labeled “Dry Mantle & Melts” is the same as in Figure 7. In Figure 8a, the grey field labeled “Sediment melt” represents mixing between mantle wedge compositions after PME (Sr/Nd and H₂O/Nd ratios of 20 and 200, respectively [Portnyagin et al., 2007; Johnson et al., 2009]) and sediment melt for the Kamchatka, Mexico, Cascades and Java arc [Plank and Langmuir, 1998] at 800–900 °C and 4.5 GPa calculated using partition coefficient values from Hermann and Rubatto [2009]. The narrow field labeled “C.A. sed. melt” represents mixing between the mantle wedge and sediment melt from Central America using the same model parameters as the other arcs. The anomalously low H₂O/Sr ratio of these sediment melts is the result of Sr-rich sediment being subducted at the trench [Plank and Langmuir, 1998]. The thick lines represent mixing between the same mantle wedge composition and AOC fluid [Bach et al., 2003] at 800 and 900 °C and 4.5 GPa calculated using partition coefficient data from Klimm et al. [2008]. Percentages of AOC fluid in the mixtures are 1%, 5%, 10% and 25%. In Figure 8b, AOC-derived fluid addition with various starting Cl concentrations is modeled in increments of 1%, 5% and 10%. See text for details of the modeling. In Figure 8c, the limits for sulfide saturation in basaltic magmas at T = 1100–1300 °C and P = 0.3–1.0 GPa are calculated from Liu et al. [2007] for an average Kawah Ijen basaltic magma (upper limit) and taken from Jugo et al. [2005] for a dry basaltic magma (lower limit). N-MORB and E-MORB compositions are calculated from the H₂O/Ce, S/Dy and Cl/K ratios reported in Saal et al. [2002] and the average N-MORB and E-MORB composition reported in Sun and McDonough [1989]. OIB is calculated in a similar fashion but element ratios are from Dixon et al. [2002], Stroncik and Haase [2004] and Workman et al. [2006]. In Figure 8d, the F/Sr ratio of fluoro-phlogopite and fluoro-apatite is from Luhr and Carmichael [1981]. The shaded field labeled “Arc potassic magmas” represents primitive shoshonitic and leucitic magmas from the western Mexican arc [Vigouroux et al., 2008].

Kawah Ijen magmas have some of the highest H₂O/Nd (63800) and Sr/Nd (46) ratios of the arc magmas considered in this study (Figure 8). Conversely, Tambora and Galunggung magmas have some of the lowest H₂O/Nd and Sr/Nd ratios; values that are only slightly above mantle values. In the case of Tambora magmas have likely experienced some H₂O degassing (Figure 4), which combined with elevated Nd contents (Figure 3), contributes to the low H₂O/Nd ratio. However, despite the potential for some underestimation of H₂O content, the low Sr/Nd ratio of these magmas, when compared to the global array, would suggest that they are inherently H₂O-poor.

[56] Addition of fluids/melts from the slab to the mantle wedge after PME is modeled in Figure 8a. Simple binary mixing of a mantle source with AOC-derived fluids at 800 or 900 °C produces trends of constant H₂O/Sr ratio (very little fractionation of H₂O-Sr-Nd occurs during mantle peridotite melting). Mixtures of a mantle source with sediment melt is also modeled at 800 and 900 °C, and the slopes of these mixing lines are noticeably different compared to those involving AOC-derived fluids. The slope of the mixing line for AOC-derived fluids at 800 °C best approximates that of the arc magmas, which is consistent with the AOC being the dominant source of Sr and H₂O in arc magmas. The variability in the H₂O/Sr ratio of the arc magmas is likely to be a combination of the following three factors: 1) variations in top of the slab temperature beneath the arcs as higher fluid H₂O/Sr ratios are produced at higher slab temperatures and lower H₂O/Sr ratios may occur at lower temperatures, although no complete compositional data is available for the lower temperature experiments; 2) variable proportions of sediment melt to AOC-derived fluids, and 3) some variability in the H₂O, Sr and Nd concentrations in the subducted components.

[57] *Mobility of Cl.* Chlorine correlates with Sr contents although to a lesser extent than H₂O. The positive correlation between Cl and H₂O [Johnson *et al.*, 2009; Ruscitto *et al.*, 2012] and Cl/Nd and Sr/Nd (Figure 8b) suggests that these elements are not significantly fractionated from each other at sub-arc depths. These ratios correlate with slab temperature (Figures 6b–6c) and the fraction of hydrous fluid/melt produced [Kessel *et al.*, 2005; Klimm *et al.*, 2008; Hermann and Rubatto, 2009]. Kawah Ijen magmas have moderate Cl/Nd and Sr/Nd ratios compared to other arc magmas, whereas Tambora magmas plot at the low end of the arc magma range. Galunggung magmas have slightly elevated Cl/Nd

ratios for a given Sr/Nd ratio compared to other arc magmas.

[58] Given the lack of experimental partitioning data for Cl between AOC or sediment and hydrous fluids/melts we cannot model the composition of subduction-derived fluids as in Figure 8a. However, we can estimate the fluid-solid bulk D value for Cl in the dehydrating meta-igneous crust to be 5–10 based on whole rock Cl contents measured in coexisting blueschist and eclogite rocks from Syros, Greece [Marschall *et al.*, 2009]. Peak metamorphic conditions for these rocks are estimated at ~2 GPa and 500 °C. We use the fluid-solid bulk D values for Nd and Sr that correspond to the lowest temperature and pressure experimental values of Kessel *et al.* (2005) and the average Sr and Nd contents of AOC from Bach *et al.* [2003]. Three different average Cl contents in the AOC were used: 50 ppm [Ito *et al.*, 1983], 200 ppm [Philippot *et al.*, 1998] and 500 ppm [Marschall *et al.*, 2009]. Based on these Cl models, the Cl/Sr ratio of arc magmas appears to correspond closely to AOC-derived fluids with a starting bulk Cl content of 200–500 ppm (Figure 8b). Note that the Cl contents in the AOC required to fit the data are higher for Galunggung and Tambora than for Kawah Ijen (500 versus 200 ppm).

[59] Although there is no obvious global correlation between the moderately-mobile elements (e.g., Th, LREE) and Cl, S and F contents (not shown), a rough correlation is seen between Cl and the LREE in some arcs (e.g., Central America [Sadofsky *et al.*, 2008]). This has been interpreted to reflect the coupled mobility of Cl (and S, F) with the LREE in the higher temperature melt phase released from the slab [Sadofsky *et al.*, 2008]. As illustrated in Figure 6a, H₂O contents are decoupled from moderately-mobile elements such as Th. This would suggest that in some arcs, Cl (and S, F) may be partly decoupled from H₂O and the hydrous fluid phase released from the slab.

[60] *Mobility of S and F.* The ratio S/Nd only weakly correlates with Sr/Nd (Figure 8c). Global variability in mantle S/REE ratios [Saal *et al.*, 2002; Workman *et al.*, 2006] and the complex speciation of sulfur in melts/fluids (see Baker and Moretti [2011] for a review) may account for this poor correlation. Most arc magmas have S contents that fall within or above the sulfide-saturation field for basaltic magmas, consistent with the high oxidation state of subduction zone magmas and the presence of S⁶⁺ along with S²⁻ in the melt [e.g., Carmichael *et al.*, 2006; Vigouroux *et al.*, 2008; Kelley and Cottrell, 2009]. Despite the elevated S solubility

limit for oxidized melts [e.g., *Jugo et al.*, 2005], we cannot discount the possibility that some magmas were saturated with respect to a S-bearing species at some point during ascent, cooling and degassing. In addition, variability in the S content of metasomatized mantle or melting of mantle containing residual sulfides could also contribute to the observed variability in S/Sr ratios of the arc magmas.

[61] Kawah Ijen magmas have S/Nd ratios that fall within the average for other calc-alkaline magmas. Tambora and Galunggung magmas have some of the lowest S/Nd ratios analysed in this study. Even though we use the least degassed S content preserved in the Tambora melt inclusions (associated with the highest H₂O content), the overall degassed nature of these melt inclusions, along with the elevated Nd values of these magmas (Figure 3), likely contributes to the low S/Nd ratio.

[62] Apart from the issue of S solubility in arc magmas, fluid sources of S to the mantle wedge may also be highly variable depending on the amount of S subducted in sediment and AOC. An average S content of ~1300 ppm is characteristic of the AOC [*Alt et al.*, 1989; *Bach et al.*, 2003], however, concentrations in sediment packages can vary greatly depending on the nature of the sediment [*Alt and Burdett*, 1982]. Pelagic clays and cherts are generally most enriched in S (1000s of ppm), whereas volcanoclastics usually have very low S contents (100s ppm [*Alt and Burdett*, 1982]). Contents for sulfur are not reported in the sediment analyses of *Plank and Langmuir* [1998], but based on the variability of sediment compositions subducted beneath arcs, highly variable S/Sr is expected in the subduction fluids/melts. Sediments subducted offshore from Kamchatka are particularly rich in pelagic clays and oozes, whereas sediments subducted off the coast of Mexico and the Cascades have a high proportion of clastic turbidites [*Plank and Langmuir*, 1998]. Average sediment subducted at the Java trench contains a mix of these sediment types. This may help explain the higher average S/Sr of the Kamchatka magmas compared to the magmas of Mexico and the Cascades. We cannot model the S/Sr ratio of these various sediment melts or of the AOC-derived fluid due to the lack of partitioning data for S.

[63] Fluorine contents do not correlate with Sr contents (Figure 8d). Tambora and other arc magmas for which we have data have F/Nd ratios similar to or slightly greater than MORB and OIB values (~20 [*Sun and McDonough*, 1989]). In contrast,

Kawah Ijen has elevated F/Nd ratios (~100). High F contents in basaltic magmas have been linked to the presence of F-rich minerals in the melting source region of these magmas (e.g., F-phlogopite [*Sigvaldason and Óskarsson*, 1986; *Vigouroux et al.*, 2008]). The F/Sr ratios of F-phlogopite and apatite from the Colima potassic magmas in western Mexico [*Luhr and Carmichael*, 1981] are shown on Figure 8d along with data from olivine-hosted melt inclusions from these potassic magmas [*Vigouroux et al.*, 2008]. The elevated F/Sr ratio of these minerals may contribute to the source of elevated F in some arc magmas. Phosphoritic sediments, rich in fluoro-apatite [e.g., *Burnett*, 1977], and F-rich aragonite and high-Mg calcite in calcareous sediments [e.g., *Kitano and Okumura*, 1973; *Wei et al.*, 2005] can also contribute to F-rich fluids/melts from the slab, however again, we lack partitioning data for F to model these fluids or melts.

5.4. Link to Subduction Zone Physical Parameters

[64] The previous section has illustrated the inverse correlation between slab surface temperature and the mobility of the most volatile (H₂O, Cl) and fluid-mobile trace elements (e.g., Sr) in subduction zones [*Plank et al.*, 2009; *Ruscitto et al.*, 2012]. The release from the slab of Sr, H₂O, Cl and to a lesser extent S, is coupled at sub-arc depths and appears to be mainly controlled by fluid release from the AOC. Experimental studies combined with thermo-mechanical models support the melt inclusion results and suggest that most sediment H₂O is released by 100 km depth, such that the AOC is the main dehydrating reservoir at sub-arc depths [*Schmidt and Poli*, 1998; *Rüpke et al.*, 2004; *Hacker*, 2008; *Johnson et al.*, 2009; *Syracuse et al.*, 2010]. We note that in certain arcs where pressure and temperature conditions in the slab are conducive to the release of water from hydrated oceanic lithospheric mantle (very hot slabs or arcs with a depth to the slab greater than ~140 km), this reservoir can also contribute to the aqueous fluid flux to the overlying sub-arc mantle [e.g., *Rüpke et al.*, 2004; *Syracuse et al.*, 2010].

[65] Among the arc volcanoes discussed in this study, the very high H₂O contents of the mantle source beneath Nicaragua [*Sadofsky et al.*, 2008] may involve the addition of H₂O released from the serpentinized mantle [*Rüpke et al.*, 2002; *Abers et al.*, 2003]. The elevated H₂O content of Kawah Ijen magmas brings into question the role of serpentinized mantle beneath the slab in eastern Java.

Offshore, deformation due to subduction of the Roo Rise results in numerous arc-parallel normal faults [Kopp *et al.*, 2006]. Flexural faulting of the plate lends support to the idea that the oceanic peridotite being subducted beneath Java may be hydrated. However, thermo-mechanical models for the Java arc suggest that despite a depth to the top of the slab of ~ 180 km, the slab may be too cold for any serpentinite dehydration [Syracuse *et al.*, 2010].

[66] For moderately hot subduction zones such as in Mexico and Central America with plate ages of 13–18 Ma [Syracuse and Abers, 2006] and a moderate slab thermal parameter (a function of the age of the slab and its vertical descent rate) of 4–11 [Syracuse *et al.*, 2010], the rate of H_2O released from the AOC reaches a maximum at a depth of less than 100 km, after which the overall flux of H_2O decreases [Schmidt and Poli, 1998; Rüpke *et al.*, 2004; Hacker, 2008; Syracuse *et al.*, 2010]. Although any correlation of magma H_2O content with distance from the trench can be complicated by temporal changes in slab geometry over time [e.g., Johnson *et al.*, 2009], the most H_2O -rich magmas in the Mexican arc are located close to the trench or inferred paleo-trench [Johnson *et al.*, 2009]. In Central America, estimates of primitive, undegassed magmatic H_2O contents are difficult to make [Sadofsky *et al.*, 2008] and any patterns with subduction zone physical parameters are harder to constrain. Nevertheless, rear-arc volcanoes from Guatemala have lower estimated primitive magma H_2O contents compared to arc-front volcanoes [Sadofsky *et al.*, 2008], as would be expected for a progressively dehydrating slab.

[67] For very young and slowly subducting plates, such as the Juan de Fuca plate currently subducting beneath Central Oregon (6 Ma [Wilson, 2002], and a low slab thermal parameter of 1–1.3 [Syracuse *et al.*, 2010]), the slab is predicted to have mostly dehydrated within the forearc region by ~ 40 km depth [Rondenay *et al.*, 2008], with waning dehydration of the slab beneath the arc [Ruscitto *et al.*, 2010]. This is consistent with the average lower H_2O content of the arc magmas [Ruscitto *et al.*, 2010].

[68] For older slabs, like the ones subducting beneath Indonesia and Kamchatka (≥ 90 Ma [Syracuse and Abers, 2006], and a slab thermal parameter of 54 [Syracuse *et al.*, 2010]), the rate of H_2O released from the AOC should be more gradual on average, with water being carried to deeper depths within the mantle [Rüpke *et al.*, 2004; Hacker, 2008; Syracuse *et al.*, 2010]. In Kamchatka, a pattern of nearly constant magmatic H_2O content across the arc is seen,

and average maximum H_2O contents, Sr/Nd and Cl/Nd ratios [Portnyagin *et al.*, 2007; Gurenko *et al.*, 2005] are lower than in the Mexican and Central American arcs, with the exception of the H_2O -rich (but relatively Cl- and Sr-poor) magmas of Klyuchevskoy volcano [Auer *et al.*, 2009] (Figure 8).

[69] Kawah Ijen has some of the highest H_2O /Nd, H_2O /Ce, Sr/Nd, Cl/Nd and S/Nd ratios of the arc magmas compared in this study, and in particular, has elevated ratios compared to magmas from other cold slab subduction zones (e.g., Kamchatka) and other magmas from the Sunda arc (Tambora and Galunggung). The recent compilation of global arc magma volatile contents and slab subduction parameters by Ruscitto *et al.* [2012] emphasizes the variability in volatile contents of primitive magmas erupted within a single arc. In comparison to Kawah Ijen, Galunggung and Tambora, also historically active and located on the volcanic front, have erupted magmas with some of the lowest H_2O /Nd and Sr/Nd ratios of any arc magmas worldwide, leading some authors to suggest a magma formation mechanism for Galunggung dominated by decompression melting as opposed to fluid-flux melting [Sisson and Bronto, 1998; Kelley *et al.*, 2006]. However, an isotopic study of Sunda arc magmas has identified a recently added ($< 8,000$ yrs) fluid component in the mantle source of the Galunggung magmas [Turner and Foden, 2001]. Although this does not preclude some decompression-induced melting in the source region of these melts, fluid fluxing is also recognized as being an important component [Turner and Foden, 2001]. Additional volatile data from Galunggung is needed to better understand the role of fluids in the generation of these magmas.

[70] The apparent variability in the proportion of hydrous fluid versus sediment melt in the Sunda arc magmas shows no simple correlation with age of the subducting plate or distance from the trench or to the top of the slab. This may reflect the complex subduction zone geometry beneath the Sunda arc. Over a similar length of arc (~ 1000 km), the Central American arc displays comparable volatile and trace element variability, which has been attributed to heterogeneous mantle sources, variations in the geometry of the subducting plate, and the nature and composition of the slab component [Eiler *et al.*, 2005; Sadofsky *et al.*, 2008]. More complete melt inclusion studies from additional Indonesian volcanoes, combined with geodynamic models of the pressure-temperature conditions of the mantle and slab beneath each volcano, are needed to map out

and understand the along-arc and across-arc pattern of H₂O release beneath the Sunda arc.

6. Conclusions

[71] From the relationship between the Sr/Nd, H₂O/Nd and Cl/Nd ratios, and the predicted composition of sediment melt and AOC-derived fluids at sub-arc depths, the dominant source of volatiles in most arc front magmas appears to be the altered oceanic crust. The contribution of sediment melt to the Sr, H₂O and Cl content in most arc magmas appears to be secondary to the AOC, although sediment melt remains important and contributes dominantly to other element fluxes such as Ba, Pb, Th and the LREE. Results from this study agree with experimental and thermo-mechanical models of fluid release in subduction zones and reinforce the role of melt inclusion studies as a complementary method for estimating the nature and relative proportion of fluid release beneath arc volcanoes. The correlation between slab surface temperature (as estimated from H₂O/Ce) and Sr/Nd suggests that Sr/Nd, in the absence of H₂O data, can act as a proxy for both the amount of AOC-derived aqueous fluid added to a given mantle source and the temperature of the slab at sub-arc depths.

[72] The source of S and F in arc magmas is not as easily discerned as for H₂O and Cl, although the moderate correlation between Sr and S contents suggests that either some S is supplied by the dehydrating AOC, or S is efficiently scavenged from the overlying metasediment layer. Highly variable S and F contents in subducted sediment, complex and poorly understood solubility mechanisms, and the lack of experimental studies on the mobility of S and F in subducted materials make it difficult to evaluate the source of these volatiles. More F analyses of melt inclusions from arc magmas and better constraints on S and F contents in slab and mantle components will improve our understanding of S and F recycling in subduction zones.

[73] Kawah Ijen, Tambora and Galunggung display different degrees of enrichment in volatile (H₂O, Cl, S, F) and highly fluid-mobile elements (Sr), with Kawah Ijen magmas recording higher AOC-derived fluid fluxes compared to Tambora and Galunggung magmas, which record higher degrees of sediment melt addition. The elevated H₂O/Ce and Sr/Nd ratios of the Kawah Ijen magmas are comparable to those from some of the most H₂O-rich magmas in

cold slab subduction zones, and are the highest yet measured in the Sunda arc.

Acknowledgments

[74] This research was supported by a NSERC-CRD grant to G. Williams-Jones and A. E. Williams-Jones. The authors would like to thank Pa Im and Jumanto for assistance in the field, as well as V. van Hinsberg, K. Berlo, S. Scher, G. Mauri, S. Palmer and numerous volunteers for their support during field work at Kawah Ijen. We also acknowledge A. Colabella's help, through the 2006 GSO SURFO program, for the collection of Tambora trace element data. Thank you to Maxim Portnyagin and Jörg Hermann for their thoughtful and constructive reviews. Assistance with microprobe analysis at the University of Oregon was provided by J. Donovan, and SIMS access at the Carnegie Institution was provided by Erik Hauri.

References

- Abers, G. A., T. Plank, and B. R. Hacker (2003), The wet Nicaraguan slab, *Geophys. Res. Lett.*, *30*(2), 1098, doi:10.1029/2002GL015649.
- Alt, J. C., and J. W. Burdett (1982), Sulfur in Pacific deep-sea sediments (leg 129) and implications for cycling of sediment in subduction zones, *Proc. Ocean Drill. Program Sci. Results*, *129*, 283–294.
- Alt, J. C., T. F. Anderson, and L. Bonnell (1989), The geochemistry of sulfur in a 1.3 km section of hydrothermally altered oceanic crust, DSDP Hole 504B, *Geochim. Cosmochim. Acta*, *53*(5), 1011–1023, doi:10.1016/0016-7037(89)90206-8.
- Alves, S., P. Schiano, and C. J. Allègre (1999), Rhenium-osmium isotopic investigation of Java subduction zone lavas, *Earth Planet. Sci. Lett.*, *168*(1–2), 65–77, doi:10.1016/S0012-821X(99)00050-3.
- Auer, S., I. Bindeman, P. J. Wallace, V. Ponomareva, and M. Portnyagin (2009), The origin of hydrous, high- $\delta^{18}\text{O}$ voluminous volcanism: Diverse oxygen isotope values and high magmatic water contents within the volcanic record of Klyuchevskoy volcano, Kamchatka, Russia, *Contrib. Mineral. Petrol.*, *157*(2), 209–230, doi:10.1007/s00410-008-0330-0.
- Bach, W., B. Peucker-Ehrenbrink, S. R. Hart, and J. S. Blusztajn (2003), Geochemistry of hydrothermally altered oceanic crust: DSDP/ODP Hole 504B—Implications for seawater-crust exchange budgets and Sr- and Pb-isotopic evolution of the mantle, *Geochem. Geophys. Geosyst.*, *4*(3), 8904, doi:10.1029/2002GC000419.
- Baker, D. R., and R. Moretti (2011), Modeling the solubility of sulfur in magmas: A 50-year old geochemical challenge, *Rev. Mineral. Geochem.*, *73*(1), 167–213, doi:10.2138/rmg.2011.73.7.
- Benjamin, E. R., T. Plank, J. A. Wade, K. A. Kelley, E. H. Hauri, and G. E. Alvarado (2007), High water contents in basaltic magmas from Irazú Volcano, Costa Rica, *J. Volcanol. Geotherm. Res.*, *168*(1–4), 68–92, doi:10.1016/j.jvolgeores.2007.08.008.
- Blundy, J., K. V. Cashman, A. Rust, and F. Witham (2010), A case for CO₂-rich arc magmas, *Earth Planet. Sci. Lett.*, *290*(3–4), 289–301, doi:10.1016/j.epsl.2009.12.013.
- Bronto, S. (1989), Volcanic geology of Galunggung, West Java, Indonesia, PhD thesis, Dep. of Geol. Sci., Univ. of Canterbury, Christchurch, New Zealand.

- Burnett, W. C. (1977), Geochemistry and origin of phosphorite deposits from off Peru and Chile, *Geol. Soc. Am. Bull.*, *88*(6), 813–823, doi:10.1130/0016-7606(1977)88<813:GAOOPD>2.0.CO;2.
- Calanchi, N., F. Lucchini, and P. L. Rossi (1983), Considerations on the high-K volcanic rocks of the volcanoes Muriah and Lasem (Java), *Mineral. Petrol. Acta*, *27*, 15–34.
- Camus, G., A. Gourgaud, P. C. Mossand-Berthommier, and P. M. Vincent (2000), Merapi (Central Java, Indonesia): An outline of the structural and magmatological evolution, with a special emphasis to the major pyroclastic events, *J. Volcanol. Geotherm. Res.*, *100*(1–4), 139–163, doi:10.1016/S0377-0273(00)00135-9.
- Carmichael, I. S. E., H. M. Frey, R. A. Lange, and C. M. Hall (2006), The Pleistocene cinder cones surrounding Volcán Colima, Mexico re-visited: Eruption ages and volumes, oxidation states, and sulfur content, *Bull. Volcanol.*, *68*(5), 407–419, doi:10.1007/s00445-005-0015-8.
- Chen, Y., A. Provost, P. Schiano, and N. Cluzel (2011), The rate of water loss from olivine-hosted melt inclusion, *Contrib. Mineral. Petrol.*, *162*(3), 625–636, doi:10.1007/s00410-011-0616-5.
- Churikova, T., G. Worner, N. Mironov, and A. Kronz (2007), Volatile (S, Cl and F) and fluid mobile trace element compositions in melt inclusions: Implications for variable fluid sources across the Kamchatka arc, *Contrib. Mineral. Petrol.*, *154*(2), 217–239, doi:10.1007/s00410-007-0190-z.
- Clements, B., R. Hall, H. R. Smyth, and M. A. Cottam (2009), Thrusting of a volcanic arc: A new structural model for Java, *Petrol. Geosci.*, *15*(2), 159–174, doi:10.1144/1354-079309-831.
- de Hoog, J. C. M., P. R. D. Mason, and M. J. Van Bergen (2001), Sulfur and chalcophile elements in subduction zones: Constraints from a laser ablation ICP-MS study of melt inclusions from Galunggung Volcano, Indonesia, *Geochim. Cosmochim. Acta*, *65*(18), 3147–3164, doi:10.1016/S0016-7037(01)00634-2.
- Dixon, J. E., and D. A. Clague (2001), Volatiles in basaltic glasses from Loihi Seamount, Hawaii: Evidence for a relatively dry plume component, *J. Petrol.*, *42*(3), 627–654, doi:10.1093/petrology/42.3.627.
- Dixon, J. E., L. Leist, C. Langmuir, and J. G. Schilling (2002), Recycled dehydrated lithosphere observed in plume-influenced mid-ocean-ridge basalt, *Nature*, *420*(6914), 385–389, doi:10.1038/nature01215.
- Edwards, C., M. Menzies, and M. Thirlwall (1991), Evidence from Muriah, Indonesia, for the interplay of supra-subduction zone and intraplate processes in the genesis of potassic alkaline magmas, *J. Petrol.*, *32*(3), 555–592.
- Edwards, C. M. H., J. D. Morris, and M. F. Thirlwall (1993), Separating mantle from slab signatures in arc lavas using B/Be and radiogenic isotope systematics, *Nature*, *362*, 530–533, doi:10.1038/362530a0.
- Edwards, C. M. H., M. A. Menzies, M. F. Thirlwall, J. D. Morris, W. P. Leeman, and R. S. Harmon (1994), The transition to potassic alkaline volcanism in island arcs: The Ringgit–Beser Complex, East Java, Indonesia, *J. Petrol.*, *35*(6), 1557–1595.
- Eiler, J. M., M. J. Carr, M. Reagan, and E. Stolper (2005), Oxygen isotope constraints on the sources of Central American arc lavas, *Geochem. Geophys. Geosyst.*, *6*, Q07007, doi:10.1029/2004GC000804.
- Feineman, M. D., F. J. Ryerson, D. J. DePaolo, and T. Plank (2007), Zoisite-aqueous fluid trace element partitioning with implications for subduction zone fluid composition, *Chem. Geol.*, *239*(3–4), 250–265, doi:10.1016/j.chemgeo.2007.01.008.
- Foden, J. (1986), The petrology of Tambora volcano, Indonesia: A model for the 1815 eruption, *J. Volcanol. Geotherm. Res.*, *27*(1–2), 1–41, doi:10.1016/0377-0273(86)90079-X.
- Foden, J. D., and R. Varne (1980), The petrology and tectonic setting of Quaternary–Recent volcanic centres of Lombok and Sumbawa, Sunda arc, *Chem. Geol.*, *30*(3), 201–226, doi:10.1016/0009-2541(80)90106-0.
- Geist, D. J., D. J. Fornari, M. D. Kurz, K. S. Harpp, S. A. Soule, M. R. Perfit, and A. M. Koleszar (2006), Submarine Fernandina: Magmatism at the leading edge of the Galapagos hot spot, *Geochem. Geophys. Geosyst.*, *7*, Q12007, doi:10.1029/2006GC001290.
- Gertisser, R., and J. Keller (2003), Trace element and Sr, Nd, Pb and O isotope variations in medium-K and high-K volcanic rocks from Merapi Volcano, Central Java, Indonesia: Evidence for the involvement of subducted sediments in Sunda Arc magma genesis, *J. Petrol.*, *44*(3), 457–489, doi:10.1093/petrology/44.3.457.
- Gertisser, R., S. Self, L. E. Thomas, H. K. Handley, P. van Calsteren, and J. A. Wolff (2012), Processes and timescales of magma genesis and differentiation leading to the great Tambora eruption in 1815, *J. Petrol.*, *53*(2), 271–297, doi:10.1093/petrology/egr062.
- Green, T. H., and J. Adam (2003), Experimentally determined trace element characteristics of aqueous fluid from partially dehydrated mafic oceanic crust at 3.0 GPa, 650–700°C, *Eur. J. Mineral.*, *15*(5), 815–830, doi:10.1127/0935-1221/2003/0015-0815.
- Gurenko, A. A., A. B. Belousov, R. B. Trumbull, and A. V. Sobolev (2005), Explosive basaltic volcanism of the Chikurachki Volcano (Kurile arc, Russia): Insights on pre-eruptive magmatic conditions and volatile budget revealed from phenocryst-hosted melt inclusions and groundmass glasses, *J. Volcanol. Geotherm. Res.*, *147*(3–4), 203–232, doi:10.1016/j.jvolgeores.2005.04.002.
- Hacker, B. R. (2008), H₂O subduction beyond arcs, *Geochem. Geophys. Geosyst.*, *9*, Q03001, doi:10.1029/2007GC001707.
- Hamilton, W. (1979), Tectonics of the Indonesian region, *U.S. Geol. Surv. Prof. Pap.*, *1078*, 345.
- Handley, H. K., C. G. Macpherson, J. P. Davidson, K. Berlo, and D. Lowry (2007), Constraining fluid and sediment contributions to subduction-related magmatism in Indonesia: Ijen Volcanic Complex, *J. Petrol.*, *48*(6), 1155–1183, doi:10.1093/petrology/egm013.
- Handley, H. K., J. P. Davidson, C. G. Macpherson, and J. A. Stimac (2008), Untangling differentiation in arc lavas: Constraints from unusual minor and trace element variations at Salak Volcano, Indonesia, *Chem. Geol.*, *255*(3–4), 360–376, doi:10.1016/j.chemgeo.2008.07.007.
- Hermann, J., and D. Rubatto (2009), Accessory phase control on the trace element signature of sediment melts in subduction zones, *Chem. Geol.*, *265*(3–4), 512–526, doi:10.1016/j.chemgeo.2009.05.018.
- Hermann, J., C. Spandler, A. Hack, and A. V. Korsakov (2006), Aqueous fluids and hydrous melts in high-pressure and ultra-high pressure rocks: Implications for element transfer in subduction zones, *Lithos*, *92*(3–4), 399–417, doi:10.1016/j.lithos.2006.03.055.
- Ito, E., D. M. Harris, and A. T. Anderson (1983), Alteration of oceanic crust and geologic cycling of chlorine and water, *Geochim. Cosmochim. Acta*, *47*(9), 1613–1624, doi:10.1016/0016-7037(83)90188-6.

- Johnson, E. R., P. J. Wallace, K. V. Cashman, H. D. Granados, and A. J. R. Kent (2008), Magmatic volatile contents and degassing-induced crystallization at Volcán Jorullo, Mexico: Implications for melt evolution and the plumbing systems of monogenetic volcanoes, *Earth Planet. Sci. Lett.*, *269*(3–4), 478–487, doi:10.1016/j.epsl.2008.03.004.
- Johnson, E. R., P. J. Wallace, H. Delgado Granados, V. C. Manea, A. J. R. Kent, I. Bindeman, and C. S. Donegan (2009), Subduction-related volatile recycling and magma generation beneath Central Mexico: Insights from melt inclusions, oxygen isotopes and geodynamic models, *J. Petrol.*, *50*(9), 1729–1764, doi:10.1093/petrology/egp051.
- Jugo, P. J., R. W. Luth, and J. P. Richards (2005), An experimental study of the sulfur content in basaltic melts saturated with immiscible sulfide or sulfate liquids at 1300°C and 1.0 GPa, *J. Petrol.*, *46*(4), 783–798, doi:10.1093/petrology/egh097.
- Kelley, K. A., and E. Cottrell (2009), Water and the oxidation state of subduction zone magmas, *Science*, *325*, 605–607, doi:10.1126/science.1174156.
- Kelley, K. A., T. Plank, J. Ludden, and H. Staudigel (2003), Composition of altered oceanic crust at ODP Sites 801 and 1149, *Geochem. Geophys. Geosyst.*, *4*(6), 8910, doi:10.1029/2002GC000435.
- Kelley, K. A., T. Plank, L. Farr, J. Ludden, and H. Staudigel (2005), Subduction cycling of U, Th, and Pb, *Earth Planet. Sci. Lett.*, *234*(3–4), 369–383, doi:10.1016/j.epsl.2005.03.005.
- Kelley, K. A., A. Colabella, T. W. Sisson, E. H. Hauri, and H. Sigurdsson (2006), Decompression melting beneath the Indonesian volcanic front, *Eos Trans. AGU*, *87*(52), Fall Meet. Suppl., Abstract V54A-03.
- Kent, A. J. R., D. W. Peate, S. Newman, E. M. Stolper, and J. A. Pearce (2002), Chlorine in submarine glasses from the Lau Basin: Seawater contamination and constraints on the composition of slab-derived fluids, *Earth Planet. Sci. Lett.*, *202*(2), 361–377, doi:10.1016/S0012-821X(02)00786-0.
- Kessel, R., M. W. Schmidt, P. Ulmer, and T. Pettke (2005), Trace element signature of subduction-zone fluids, melts and supercritical liquids at 120–180 km depth, *Nature*, *437*, 724–727, doi:10.1038/nature03971.
- Kitano, Y., and M. Okumura (1973), Coprecipitation of fluoride with calcium carbonate, *Geochem. J.*, *7*, 37–49, doi:10.2343/geochemj.7.37.
- Klimm, K., J. D. Blundy, and T. H. Green (2008), Trace element partitioning and accessory phase saturation during H₂O-saturated melting of basalt with implications for subduction zone chemical fluxes, *J. Petrol.*, *49*(3), 523–553, doi:10.1093/petrology/egn001.
- Kohut, E. J., R. J. Stern, A. J. R. Kent, R. L. Nielsen, S. H. Bloomer, and M. Leybourne (2006), Evidence for adiabatic decompression melting in the Southern Mariana Arc from high-Mg lavas and melt inclusions, *Contrib. Mineral. Petrol.*, *152*(2), 201–221, doi:10.1007/s00410-006-0102-7.
- Kopp, H., E. R. Flueh, C. J. Petersen, W. Weinrebe, A. Wittwer, and Meramex Scientists (2006), The Java margin revisited: Evidence for subduction erosion off Java, *Earth Planet. Sci. Lett.*, *242*(1–2), 130–142, doi:10.1016/j.epsl.2005.11.036.
- Kuno, H. (1960), High-alumina basalt, *J. Petrol.*, *1*(2), 121–145.
- Lehnert, K., Y. Su, C. H. Langmuir, B. Sarbas, and U. Nohl (2000), A global geochemical database structure for rocks, *Geochem. Geophys. Geosyst.*, *1*(5), 1012, doi:10.1029/1999GC000026.
- Liu, Y., N. T. Samaha, and D. R. Baker (2007), Sulfur concentration at sulfide saturation (SCSS) in magmatic silicate melts, *Geochim. Cosmochim. Acta*, *71*(7), 1783–1799, doi:10.1016/j.gca.2007.01.004.
- Luhr, J. F., and I. S. E. Carmichael (1981), The Colima volcanic complex, Mexico: Part II. Late-quaternary cinder cones, *Contrib. Mineral. Petrol.*, *76*(2), 127–147, doi:10.1007/BF00371954.
- Marschall, H. R., R. Altherr, and L. Rüpke (2007), Squeezing out the slab—modeling the release of Li, Be and B during progressive high-pressure metamorphism, *Chem. Geol.*, *239*(3–4), 323–335, doi:10.1016/j.chemgeo.2006.08.008.
- Marschall, H. R., R. Altherr, K. Gmélting, and Z. Kasztovszky (2009), Lithium, boron and chlorine as tracers for metasomatism in high-pressure metamorphic rocks: A case study from Syros (Greece), *Mineral. Petrol.*, *95*(3–4), 291–302, doi:10.1007/s00710-008-0032-3.
- Nadeau, O., A. E. Williams-Jones, and J. Stix (2010), Sulphide magma as a source of metals in arc-related magmatic hydrothermal ore fluids, *Nat. Geosci.*, *3*, 501–505, doi:10.1038/ngeo899.
- Newman, S., and J. B. Lowenstern (2002), VolatileCalc: A silicate melt-H₂O-CO₂ solution model written in Visual Basic for Excel, *Comput. Geosci.*, *28*, 597–604, doi:10.1016/S0098-3004(01)00081-4.
- Nicholls, I. A., and D. J. Whitford (1983), Potassium-rich volcanic rocks of the Muriah complex, Java, Indonesia: Products of multiple magma sources?, *J. Volcanol. Geotherm. Res.*, *18*(1–4), 337–359, doi:10.1016/0377-0273(83)90015-X.
- Papale, P., R. Moretti, and D. Barbato (2006), The compositional dependence of the saturation surface of H₂O + CO₂ fluids in silicate melts, *Chem. Geol.*, *229*(1–3), 78–95, doi:10.1016/j.chemgeo.2006.01.013.
- Pearce, J. A., and D. W. Peate (1995), Tectonic implications of the composition of volcanic arc magmas, *Annu. Rev. Earth Planet. Sci.*, *23*, 251–285, doi:10.1146/annurev.ea.23.050195.001343.
- Peccerillo, A., and S. R. Taylor (1976), Geochemistry of Eocene calc-alkaline volcanic rocks from the Kastamonu area, northern Turkey, *Contrib. Mineral. Petrol.*, *58*(1), 63–81, doi:10.1007/BF00384745.
- Philippot, P., P. Agrinier, and M. Scambelluri (1998), Chlorine cycling during subduction of altered oceanic crust, *Earth Planet. Sci. Lett.*, *161*(1–4), 33–44, doi:10.1016/S0012-821X(98)00134-4.
- Plank, T. (2005), Constraints from thorium/lanthanum on sediment recycling at subduction zones and the evolution of the continents, *J. Petrol.*, *46*(5), 921–944, doi:10.1093/petrology/egi005.
- Plank, T., and C. H. Langmuir (1993), Tracing trace elements from sediment input to volcanic output at subduction zones, *Nature*, *362*, 739–743, doi:10.1038/362739a0.
- Plank, T., and C. H. Langmuir (1998), The chemical composition of subducting sediment and its consequences for the crust and mantle, *Chem. Geol.*, *145*(3–4), 325–394, doi:10.1016/S0009-2541(97)00150-2.
- Plank, T., L. B. Cooper, and C. E. Manning (2009), Emerging geothermometers for estimating slab surface temperatures, *Nat. Geosci.*, *2*(9), 611–615, doi:10.1038/ngeo614.
- Portnyagin, M., K. Hoernle, P. Plechov, N. Mironov, and S. Khubunaya (2007), Constraints on mantle melting and composition and nature of slab components in volcanic arcs from volatiles (H₂O, S, Cl, F) and trace elements in melt inclusions from the Kamchatka Arc, *Earth Planet. Sci. Lett.*, *255*(1–2), 53–69, doi:10.1016/j.epsl.2006.12.005.
- Portnyagin, M., R. Almeev, S. Matveev, and F. Holtz (2008), Experimental evidence for rapid water exchange between melt inclusions in olivine and host magma, *Earth Planet. Sci. Lett.*, *272*(3–4), 541–552, doi:10.1016/j.epsl.2008.05.020.

- Reagan, M. K., O. Ishizuka, R. J. Stern, K. A. Kelley, Y. Ohara, J. Blichert-Toft, S. H. Bloomer, J. Cash, P. Fryer, and B. B. Hanan (2010), Fore-arc basalts and subduction initiation in the Izu-Bonin-Mariana system, *Geochem. Geophys. Geosyst.*, *11*, Q03X12, doi:10.1029/2009GC002871.
- Reubi, O., and I. A. Nicholls (2004), Magmatic evolution at Batur volcanic field, Bali, Indonesia: Petrological evidence for polybaric fractional crystallization and implications for caldera-forming eruptions, *J. Volcanol. Geotherm. Res.*, *138*(3–4), 345–369, doi:10.1016/j.jvolgeores.2004.07.009.
- Reubi, O., I. A. Nicholls, and V. S. Kamenetsky (2003), Early mixing and mingling in the evolution of basaltic magmas: Evidence from phenocryst assemblages, Slamet Volcano, Java, Indonesia, *J. Volcanol. Geotherm. Res.*, *119*(1–4), 255–274, doi:10.1016/S0377-0273(02)00357-8.
- Roberge, J., H. Delgado-Granados, and P. J. Wallace (2009), Mafic magma recharge supplies high CO₂ and SO₂ gas fluxes from Popocatepetl volcano, Mexico, *Geology*, *37*(2), 107–110, doi:10.1130/G25242A.1.
- Rondenay, S., G. A. Abers, and P. E. van Keken (2008), Seismic imaging of subduction zone metamorphism, *Geology*, *36*(4), 275–278, doi:10.1130/G24112A.1.
- Rowe, M. C., A. J. R. Kent, and R. L. Nielsen (2009), subduction influence on oxygen fugacity and trace and volatile elements in basalts across the cascade volcanic arc, *J. Petrol.*, *50*(1), 61–91, doi:10.1093/petrology/egn072.
- Rüpke, L. H., J. P. Morgan, M. Hort, and J. A. D. Connolly (2002), Are the regional variations in Central American arc lavas due to differing basaltic versus peridotitic slab sources of fluids?, *Geology*, *30*(11), 1035–1038, doi:10.1130/0091-7613(2002)030<1035:ATRVIC>2.0.CO;2.
- Rüpke, L. H., J. P. Morgan, M. Hort, and J. A. D. Connolly (2004), Serpentine and the subduction zone water cycle, *Earth Planet. Sci. Lett.*, *223*(1–2), 17–34, doi:10.1016/j.epsl.2004.04.018.
- Ruscitto, D. M., P. J. Wallace, E. R. Johnson, A. J. R. Kent, and I. N. Bindeman (2010), Volatile contents of mafic magmas from cinder cones in the Central Oregon High Cascades: Implications for magma formation and mantle conditions in a hot arc, *Earth Planet. Sci. Lett.*, *298*(1–2), 153–161, doi:10.1016/j.epsl.2010.07.037.
- Ruscitto, D. M., P. J. Wallace, L. B. Cooper, and T. Plank (2012), Global variations in H₂O/Ce II: Relationships to arc magma geochemistry and volatile fluxes, *Geochem. Geophys. Geosyst.*, *13*, Q03025, doi:10.1029/2011GC003887.
- Saal, A. E., E. H. Hauri, C. H. Langmuir, and M. R. Perfit (2002), Vapor undersaturation in primitive mid-ocean-ridge basalt and the volatile content of Earth's upper mantle, *Nature*, *419*(6906), 451–455, doi:10.1038/nature01073.
- Sadofsky, S. J., M. Portnyagin, K. Hoernle, and P. van den Bogaard (2008), Subduction cycling of volatiles and trace elements through the Central American volcanic arc: Evidence from melt inclusions, *Contrib. Mineral. Petrol.*, *155*(4), 433–456, doi:10.1007/s00410-007-0251-3.
- Salters, V. J. M., and A. Stracke (2004), Composition of the depleted mantle, *Geochem. Geophys. Geosyst.*, *5*, Q05B07, doi:10.1029/2003GC000597.
- Scambelluri, M., O. Müntener, L. Ottolini, T. T. Pettke, and R. Vannucci (2004), The fate of B, Cl and Li in the subducted oceanic mantle and in the antigorite breakdown fluids, *Earth Planet. Sci. Lett.*, *222*(1), 217–234, doi:10.1016/j.epsl.2004.02.012.
- Schiano, P., J. M. Eiler, I. D. Hutcheon, and E. M. Stolper (2000), Primitive CaO-rich, silica-undersaturated melts in island arcs: Evidence for the involvement of clinopyroxene-rich lithologies in the petrogenesis of arc magmas, *Geochem. Geophys. Geosyst.*, *1*(5), 1018, doi:10.1029/1999GC000032.
- Schmidt, M. W., and S. Poli (1998), Experimentally based water budgets for dehydrating slabs and consequences for arc magma generation, *Earth Planet. Sci. Lett.*, *163*(1–4), 361–379, doi:10.1016/S0012-821X(98)00142-3.
- Self, S., M. R. Rampino, M. S. Newton, and J. A. Wolf (1984), Volcanological study of the great Tambora eruption of 1815, *Geology*, *12*(11), 659–663, doi:10.1130/0091-7613(1984)12<659:VSOTGT>2.0.CO;2.
- Sendjaja, Y. A., J. I. Kimura, and E. Sunardi (2009), Across-arc geochemical variation of Quaternary lavas in West Java, Indonesia: Mass-balance elucidation using arc basalt simulator model, *Isl. Arc*, *18*(1), 201–224, doi:10.1111/j.1440-1738.2008.00641.x.
- Siebert, L., and T. Simkin (2002), *Volcanoes of the World: An Illustrated Catalog of Holocene Volcanoes and Their Eruptions*, *Global Volcanism Digital Inf. Ser.*, GVP- 3, Smithsonian Inst., Washington, D. C. [Available online at <http://www.volcano.si.edu/world/>].
- Sigurdsson, H., and S. Carey (1992), Eruptive history of Tambora volcano, Indonesia, *Mitt. Geol. Palaeontol. Inst. Univ. Hamburg*, *70*, 187–206.
- Sigvaldason, G. E., and N. Óskarsson (1986), Fluorine in basalts from Iceland, *Contrib. Mineral. Petrol.*, *94*(3), 263–271, doi:10.1007/BF00371435.
- Sisson, T. W., and S. Bronto (1998), Evidence for pressure-release melting beneath arcs from basalt at Galunggung, Indonesia, *Nature*, *391*, 883–886, doi:10.1038/36087.
- Sitorus, K. (1990), Volcanic stratigraphy and geochemistry of the Idjen Caldera Complex, East Java, Indonesia, MSc thesis, School of Geogr., Environ. and Earth Sci., Victoria Univ. of Wellington, Wellington, New Zealand.
- Smyth, H. R., P. J. Hamilton, R. Hall, and P. D. Kinny (2007), The deep crust beneath island arcs: Inherited zircons reveal a Gondwana continental fragment beneath East Java, Indonesia, *Earth Planet. Sci. Lett.*, *258*(1–2), 269–282, doi:10.1016/j.epsl.2007.03.044.
- Spilliaert, N., N. Métrich, and P. Allard (2006), S-Cl-F degassing pattern of water-rich alkali basalt: Modeling and relationship with eruption styles on Mount Etna volcano, *Earth Planet. Sci. Lett.*, *248*(3–4), 772–786, doi:10.1016/j.epsl.2006.06.031.
- Stroncik, N. A., and K. M. Haase (2004), Chlorine in oceanic intraplate basalts: Constraints on mantle sources and recycling processes, *Geology*, *32*(11), 945–948, doi:10.1130/G21027.1.
- Sun, S. S., and W. F. McDonough (1989), Chemical and isotopic systematics of oceanic basalts: Implications for mantle composition and processes, *Geol. Soc. Spec. Publ.*, *42*(1), 313–345, doi:10.1144/GSL.SP.1989.042.01.19.
- Syracuse, E. M., and G. A. Abers (2006), Global compilation of variations in slab depth beneath arc volcanoes and implications, *Geochem. Geophys. Geosyst.*, *7*, Q05017, doi:10.1029/2005GC001045.
- Syracuse, E. M., P. E. van Keken, and G. A. Abers (2010), The global range of subduction zone thermal models, *Phys. Earth Planet. Int.*, *183*(1–2), 73–90, doi:10.1016/j.pepi.2010.02.004.
- Tenthorey, E., and J. Hermann (2004), Composition of fluids during serpentinite breakdown in subduction zones: Evidence for limited boron mobility, *Geology*, *32*(10), 865–868, doi:10.1130/G20610.1.
- Tollstrup, D., J. Gill, A. J. R. Kent, D. Prinkey, R. Williams, Y. Tamura, and O. Ishizuka (2010), Across-arc geochemical trends in the Izu-Bonin arc: Contributions from the subducting

- slab, revisited, *Geochem. Geophys. Geosyst.*, *11*, Q01X10, doi:10.1029/2009GC002847.
- Tregoning, P., F. K. Brunner, Y. Bock, S. S. O. Puntodewo, R. McCaffrey, J. F. Genrich, E. Calais, J. Rais, and C. Subarya (1994), First geodetic measurement of convergence across the Java trench, *Geophys. Res. Lett.*, *21*(19), 2135–2138, doi:10.1029/94GL01856.
- Turner, S., and J. D. Foden (2001), U, Th and Ra disequilibria, Sr, Nd and Pb isotope and trace element variations in Sunda arc lavas: Predominance of a subducted sediment component, *Contrib. Mineral. Petrol.*, *142*(1), 43–57, doi:10.1007/s004100100271.
- van Hinsberg, V. (2001), Water-rock interaction and element fluxes in the Kawah Ijen hyperacid crater lake and the Banyu Pait river, East Java, Indonesia, MSc thesis, Dep. of Earth Sci., Univ. of Utrecht, Utrecht, Netherlands.
- Vigouroux, N. (2011), Tracking the evolution of magmatic volatiles from the mantle to the atmosphere using integrative geochemical and geophysical methods, PhD thesis, Dep. of Earth Sci., Simon Fraser Univ., Burnaby, B. C., Canada.
- Vigouroux, N., P. J. Wallace, and A. J. R. Kent (2008), Volatiles in high-K magmas from the Western Trans-Mexican Volcanic Belt: Evidence for fluid fluxing and extreme enrichment of the mantle wedge by subduction processes, *J. Petrol.*, *49*(9), 1589–1618, doi:10.1093/ptrology/egn039.
- Vlastélic, I., A. Peltier, and T. Staudacher (2007), Short term (1998–2006) fluctuations of Pb isotopes at Piton de la Fournaise volcano (Reunion Island): Origins and constraints on the size and shape of the magma reservoir, *Chem. Geol.*, *244*(1–2), 202–220, doi:10.1016/j.chemgeo.2007.06.015.
- Vukadinovic, D., and I. Sutawidjaja (1995), Geology, mineralogy and magma evolution of Gunung Slamet volcano, Java, Indonesia, *J. Southeast Asian Earth Sci.*, *11*(2), 135–164, doi:10.1016/0743-9547(94)00043-E.
- Wade, J. A., T. Plank, W. G. Melson, G. J. Soto, and E. H. Hauri (2006), The volatile content of magmas from Arenal volcano, Costa Rica, *J. Volcanol. Geotherm. Res.*, *157*(1–3), 94–120, doi:10.1016/j.jvolgeores.2006.03.045.
- Wallace, P. J. (2005), Volatiles in subduction zone magmas: Concentrations and fluxes based on melt inclusion and volcanic gas data, *J. Volcanol. Geotherm. Res.*, *140*(1–3), 217–240, doi:10.1016/j.jvolgeores.2004.07.023.
- Weaver, S. L., P. J. Wallace, and A. D. Johnston (2011), A comparative study of continental vs. intraoceanic arc mantle melting: Experimentally determined phase relations of hydrous primitive melts, *Earth Planet. Sci. Lett.*, *308*(1–2), 97–106, doi:10.1016/j.epsl.2011.05.040.
- Wei, W., M. Kastner, A. Deyhle, and A. J. Spivack (2005), Geochemical cycling of fluorine, chlorine, bromine, and boron and implications for fluid-rock reactions in Mariana Forearc, South Chamorro Seamount, ODP Leg 195, *Proc. Ocean Drill. Program Sci. Results*, *195*, 1–23.
- Wheller, G. E., R. Varne, J. D. Foden, and M. J. Abbott (1987), Geochemistry of quaternary volcanism in the Sunda-Banda arc, Indonesia, and three-component genesis of island-arc basaltic magmas, *J. Volcanol. Geotherm. Res.*, *32*(1–3), 137–160, doi:10.1016/0377-0273(87)90041-2.
- Whitford, D. J., I. A. Nicholls, and R. S. Taylor (1979), Spatial variations in the geochemistry of quaternary lavas across the Sunda arc in Java and Bali, *Contrib. Mineral. Petrol.*, *70*(3), 341–356, doi:10.1007/BF00375361.
- Wilson, D. S. (2002), The Juan de Fuca plate and slab—Isochron structure and Cenozoic plate motions, *U.S. Geol. Surv. Open-File Rep.*, *02-328*, 9–12.
- Workman, R. K., and S. R. Hart (2005), Major and trace element composition of the depleted MORB mantle (DMM), *Earth Planet. Sci. Lett.*, *231*(1–2), 53–72, doi:10.1016/j.epsl.2004.12.005.
- Workman, R. K., E. Hauri, S. R. Hart, J. Wang, and J. Blusztajn (2006), Volatile and trace elements in basaltic glasses from Samoa: Implications for water distribution in the mantle, *Earth Planet. Sci. Lett.*, *241*(3–4), 932–951, doi:10.1016/j.epsl.2005.10.028.
- Wyszczanski, R. J., I. C. Wright, J. A. Gamble, E. H. Hauri, J. F. Luhr, S. M. Eggins, and M. R. Handler (2006), Volatile contents of Kermadec Arc-Havre Trough pillow glasses: Fingerprinting slab-derived aqueous fluids in the mantle sources of arc and back-arc lavas, *J. Volcanol. Geotherm. Res.*, *152*(1–2), 51–73, doi:10.1016/j.jvolgeores.2005.04.021.